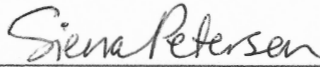
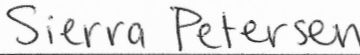
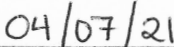








Jacob Okun

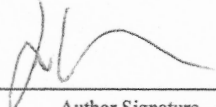
Significant Intensification of Eastern Pacific ENSO reflected in Galápagos Corals since the Pre-Industrial Era: A Synthesis of New and Published Fossil Coral Cores from the Tropical Eastern and Central Pacific Ocean

submitted in partial fulfillment of the requirements for the degree of
Master of Science in Earth and Environmental Sciences
Department of Earth and Environmental Sciences
The University of Michigan

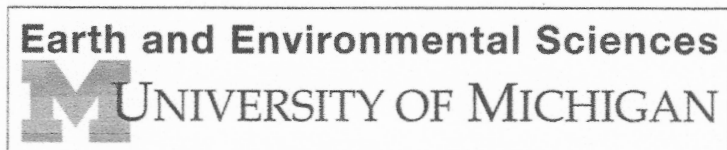
 _____	Accepted by:  _____	 _____
	Name	Date
 _____	 _____	 _____
Signature	Name	Date
 _____	 _____	 _____
Department Chair Signature	Name	Date

I hereby grant the University of Michigan, its heirs and assigns, the non-exclusive right to reproduce and distribute single copies of my thesis, in whole or in part, in any format. I represent and warrant to the University of Michigan that the thesis is an original work, does not infringe or violate any rights of others, and that I make these grants as the sole owner of the rights to my thesis. I understand that I will not receive royalties for any reproduction of this thesis.

- Permission granted.
 Permission granted to copy after: _____
 Permission declined.



Author Signature



Significant Intensification of Eastern Pacific ENSO reflected in Galápagos Corals since the Pre-Industrial Era: A Synthesis of New and Published Fossil Coral Cores from the Tropical Eastern and Central Pacific Ocean

by

Jacob M. Okun, Julia E. Cole, Diane M. Thompson, Allison E. Lawman, Kelsey Dyez, Emma Reed, Gloria Jimenez, Anson Cheung, Alexander W. Tudhope, R. Lawrence Edwards

A dissertation submitted in partial fulfillment
of the requirements for the degree of Master of Science
(Earth and Environmental Science)
in The University of Michigan
2021

Committee:

Professor Julia E. Cole, Advisor
Professor Sierra V. Petersen, Co-Reader
Professor Marin Clark, EARTH Chair, Co-Reader

Jacob M. Okun

jakeokun@umich.edu

ORCID iD: 0000-0001-7902-9786

TABLE OF CONTENTS

LIST OF TABLES	v
ABSTRACT	vi-vii
INTRODUCTION	1
El Niño Southern Oscillation (ENSO)	2
Paleoclimate Context	3
Eastern Pacific Sites	5
METHODS	7
EP Site Description	7
New $\delta^{18}\text{O}$ Records from Genovesa Island	8
Reprocessing Published Coral Paleorecords	9
20 th Century Coral Records	10
DATA PROCESSING	11
Defining Intervals for Comparison	13
RESULTS	14
New/Reprocessed Fossil EP Age Dates and Record Lengths	14
Bandpass Filtering/Standard Deviation Method	14
High-pass/PDF Method	15
DISCUSSION	16
EP ENSO Variability	16

CP ENSO Variability	17
Other EP and Tropical Pacific Paleoclimate Data	18
Is EP ENSO Intensification a Response to Anthropogenic Greenhouse Forcing?	19
CONCLUSIONS	22
BIBLIOGRAPHY	24
FIGURES	32
SUPPLEMENTARY MATERIAL	40

LIST OF TABLES

TABLE

S.1	55-57
S.2	58
S.3	59-60

ABSTRACT

El Niño Southern Oscillation (ENSO), and its potential response to anthropogenic climate change, has recently become a topic of great interest following the anomalously strong El Niño events of the late 20th-early 21st centuries. Strong events such as these are associated with drought, flooding, and damages to ecosystems, human health, agriculture, and infrastructure in many parts of the world. Long-lived corals in the equatorial Pacific Ocean track ENSO-related sea surface temperature (SST) over time in the Sr/Ca and oxygen isotopic ratios ($d^{18}O$) of their skeletons, and these multi-decadal to multi-century histories can be accessed at monthly resolution. SST anomalies can be reconstructed from well-dated subfossil corals, providing “windows” into past ENSO activity. Current ENSO trends can be assessed by comparing past (pre-industrial) and modern windows of variability. The 17th-18th centuries, within a period of cooler temperatures in the northern hemisphere (the so-called “Little Ice Age”), provide a climatologically interesting window, as previously published records from the central Pacific suggest high ENSO variability at this time. Here, we investigate central Pacific (CP) and eastern Pacific (EP) ENSO variability using new and published subfossil coral records from the 17th-18th centuries, and compare them to the 20th century, as well as to the “recent modern” interval of 1990-2010 CE. We find that in the EP, El Niño variability has increased substantially since the 1600’s, particularly in the recent modern interval. This result contrasts with CP variability, which we find does not change substantially over the past 400 years. Our new Galápagos coral records demonstrate that ENSO in the EP is intensifying, in line with model projections under

anthropogenic forcing and with the limited instrumental record. Such amplification will likely intensify the global impacts of the ENSO system in a warming world.

INTRODUCTION

Interannual climate extremes associated with the El Niño-Southern Oscillation (ENSO) system are among the leading causes of climate disasters (Goddard and Dilley, 2005; Goddard and Gershunov 2021; McPhaden et al., 2021), and the unresolved questions around ENSO's response to enhanced greenhouse forcing continue to motivate a tremendous research effort (McPhaden et al. 2021). ENSO is the largest source of interannual climate variability on the planet, characterized by interannual oscillations between cool and warm sea surface temperature anomalies (SSTAs) in the tropical Pacific, and concurrent rearrangements of the trade wind, convection, and ocean circulation fields. Recent work has explored whether enhanced greenhouse forcing in the modern era is causing ENSO to become stronger and more variable (e.g., Cai et al. 2015; Emile-Geay et al., 2016; McPhaden et al., 2021), or changing the spatial characteristics of ENSO (e.g., Yeh et al., 2009; Newman et al., 2011; Capotondi et al., 2013; 2015). Some have suggested that extreme ENSO events could occur twice as frequently by the end of the 21st century under current rates of greenhouse gas emissions (Cai et al., 2014; 2015). Others highlight the difficulty in distinguishing a forced signal from ENSO's naturally large internal variability, as represented in unforced model simulations displaying ENSO's spatial and temporal variability over time (Wittenberg, 2009; Vecchi and Wittenberg, 2010; Newman et al., 2011). Paleoclimate data provide valuable points of comparison for long model simulations and suggest that real-world modern variability exceeds the range of the past millennium (Grothe et

al. 2019; Emile-Geay et al. 2021). Here we synthesize new and published data from eastern Pacific (Galápagos) corals that adds to our understanding of pre-industrial ENSO variance.

El Niño Southern Oscillation (ENSO)

ENSO describes an interannual ocean-atmosphere phenomenon that occurs on a scale of 2-7 years and spans the tropical Pacific Ocean. During El Niño, the “warm phase” of ENSO, weak trade winds reduce upwelling of cool water in the eastern Pacific Ocean and allow anomalously warm waters to spread across the equatorial Pacific. The opposite trend is true of La Niña events, the “cold phase” of ENSO, when strengthened trade winds increase upwelling, creating cooler temperatures. Extreme ENSO events have potentially dire global climatic and environmental consequences (e.g., McPhaden et al., 2006; Yeh et al., 2018). In the last century, some of the strongest El Niño events on record have occurred (1982-3, 1997-8, 2015-16; Santoso et al., 2017), and many parts of the world experienced adverse effects pertaining to agriculture, drought/flood frequency, and human health (Zhang et al., 1996; Trenberth et al., 1998; Kovats, 2000; Ribsey et al., 2009; Santoso et al., 2017; McPhaden et al., 2021). These impacts warrant analysis of trends in ENSO’s behavior and variability, to estimate whether anomalous events should be expected more frequently in the future under growing anthropogenic greenhouse forcing.

Although El Niño events were initially identified in the eastern Pacific (EP; Bjerknes, 1969; Rasmusson and Carpenter 1982), recent observations extending across the full tropical Pacific have revealed a second pattern of El Niño in which warming is concentrated in the central Pacific (CP; Fig. 1; e.g., Larkin and Harrison, 2005; Ashok et al., 2007; Kao and Yu,

2009; Kug et al., 2009; Yeh et al., 2009; Newman et al., 2011; Takahashi et al., 2011; Capotondi et al., 2013; 2015). Occurrences of this CP El Niño, also known as a dateline El Niño (Larkin and Harrison, 2005), El Niño Modoki (Ashok et al., 2007), or warm pool El Niño (Kug et al., 2009), appear to be increasing relative to EP events. The increasing CP/EP event ratio is associated with a steepening thermocline and strengthening Walker circulation across the tropical Pacific (Cai et al., 2018; Heede et al., 2020). Initially hypothesized as a consequence of anthropogenic warming (Yeh et al. 2009), long climate model integrations suggest that this spatial variability may also result from random weather forcing as part of ENSO's large internal variability (Newman et al., 2011; Yeh et al 2011). Whether the increased prevalence of CP anomalies results from external forcing or internal variability remains a topic of active debate (Capotondi et al., 2021).

Paleoclimate Context

Anticipating future changes in ENSO is challenging, in part because we lack extensive data on the preindustrial (unforced/naturally forced) range of ENSO variability in spatial pattern, intensity, and frequency. To identify ENSO trends, we require observations that span before and after the Industrial Revolution to evaluate the influence of greenhouse gas emissions and anthropogenic warming. Since instrumental records of tropical Pacific SST are short and sparse before the mid-20th century (Deser et al., 2010), paleoclimate records can be used to investigate longer-term variability (Emile-Geay et al. 2021 and references therein). Corals are particularly appropriate for this task as they preserve multi-decadal to multi-century histories of SST in their skeletal geochemistry that can be accessed at monthly resolution.

Long-lived corals track ENSO-related SST over time in the Sr/Ca and oxygen isotopic ratios ($\delta^{18}\text{O}$) of their skeletons (e.g., Dunbar et al., 1994; Cobb et al., 2013; Cole and Tudhope, 2017; Jimenez et al. 2018; Grothe et al. 2019; Sanchez et al. 2020). Coral $\delta^{18}\text{O}$ reflects the combined influence of SST (via a thermodynamic fractionation factor; Epstein et al. 1953), the $\delta^{18}\text{O}$ of seawater (usually proportional to salinity; Conroy et al. 2017), and a biological offset factor (Weber and Woodhead 1972). Warmer SSTs correlate with relatively negative $\delta^{18}\text{O}$ values in corals. Coral Sr/Ca also correlates inversely with SST and may be advantageous in that salinity variations do not impact these records (Beck et al., 1992; Wu et al., 2013; Moreau et al. 2015; Jimenez et al., 2018). Records from living coral colonies can span centuries (as summarized in Cole et al., 2002; Lough, 2004; Emile-Geay et al. 2021), and opportunistic sampling of fossil material provides multidecadal or longer paleoclimate “windows” (SST records spanning a designated period of years in the past) that extend our perspective back in time (e.g., Tudhope et al. 2001; Cobb et al., 2003; 2013; Grothe et al., 2019; Lawman et al. 2020). Several studies have compiled modern records to produce reconstructions of ENSO-related indices, and the biases associated with this work are becoming clarified (e.g., McGregor et al., 2013; Emile-Geay et al., 2016; Freund et al., 2019; Loope et al., 2020).

In several paleoclimate studies of pre-industrial tropical variability, the interval around the 1700’s CE stands out for high variability. Cobb et al. (2003) first noted this in corals from Palmyra, a result that held up in subsequent analyses of these data (Cobb et al. 2013; Grothe et al. 2019). Freund et al. (2019), using a network of coral sites that includes Palmyra, reconstruct strong CP ENSO variance in the 17th century; this result likely reflects the contribution of the Palmyra record to this data-sparse interval. Using corals from the eastern Indian Ocean, Abram

et al. (2020) find similarly enhanced variance in the 17th century, and summarize evidence for additional anomalies across the Indo-Pacific monsoon domain. Using marine sediment data, Rustic et al. (2015) point to a reduced zonal Pacific SST gradient at this time, indicating weaker Walker circulation, warmer equatorial conditions, and a prolonged “El Niño-like” state; they also note higher SST variance, based on individual foraminifera analysis of $\delta^{18}\text{O}$. The reduced zonal Pacific SST gradient and El Niño-like conditions coincide with a southward positioning of the Inter-Tropical Convergence Zone (ITCZ), inferred during the 17th-18th centuries based on hydrogen isotopic evidence from Galápagos lake sediments (Sachs et al., 2009). While the cause of this southward shift is debated, one theory attributes the shift to high atmospheric aerosol concentrations, a consequence of enhanced volcanic activity during this time period (Yan et al., 2015). Yan et al. (2015) provide paleorecords and model data suggesting an enhanced Asian-Australian Monsoon during the 17th-18th centuries that was shifted toward the tropics, consistent with a southward shift of the ITCZ. Taken together, the 17th-18th centuries appear to have experienced highly variable and warm (potentially El Niño-dominated) conditions across the Indo-Pacific tropics. This interpretation is particularly interesting given the tendency for generally cool conditions globally, as part of the so-called “Little Ice Age” (e.g., Mann et al. 2009).

Eastern Pacific Sites

This work focuses on a new suite of records from the Galápagos archipelago (Ecuador), including modern and preindustrial intervals. The eastern tropical Pacific remains poorly sampled in terms of long coral paleoclimate data (Tierney et al. 2015). Many of the first coral paleoclimate advances used corals from the Galápagos (e.g., McConnaughey et al. 1989; Shen et

al. 1987; Lea et al. 1989; Dunbar et al. 1994; Schrag et al. 1999; Cole and Tudhope 2017).

However, the development of long, subseasonal records has been hampered by the challenging conditions for coral growth in the upwelling waters of the EP, including the widespread mortality of Galápagos corals in the 1982-3 and 1997-8 El Niño events (Glynn et al. 2009) that terminate most coral records between 1981 and 1983 CE. Our analysis uses modern corals from the northern Galápagos, where corals recovered from the strong events of the late 20th century and continued growing to present (Glynn et al. 2015; Jimenez et al. 2018); we compare these with subfossil corals from several islands across the archipelago that date to the 17th-18th centuries.

The EP is a critical node of the ENSO system. The most intense tropical Pacific upwelling occurs off the western coast of South America, near the Galápagos region (Wang et al., 2017). During El Niño events, eastern upwelling is suppressed due to weakened trade winds. Warm water from the western Pacific extends further east as the thermocline deepens. These warm SSTAs are clearly captured in the geochemistry of Galápagos corals, which normally experience cooler, upwelled water. This site is the only island group within the core EP-ENSO region and provides a key counterpoint to the extensive work in the Line Islands (CP-ENSO). Here we describe two new 17th-18th century coral SST records from Genovesa Island, and we update a published record from Wolf Island (Reed et al. 2021) and published data from Urvina Bay, Isabela Island (Druffel et al. 2015; Fig. 2; Fig. 3). These records allow us to explore how ENSO variability in the EP behaved during this preindustrial interval of unusual behavior in the CP and tropical Indian Ocean.

METHODS

EP Site Description

The Galápagos Islands make up a volcanic archipelago in the eastern Pacific Ocean, approximately 1000 km (600 miles) off the western coast of South America (Fig. 2). At the largest and westernmost island, Isabela, the equatorial undercurrent strikes the Galápagos platform, creating the coolest and most variable conditions in the archipelago; these upwelled waters spread throughout the remaining smaller islands to the north- and southeast. The Galápagos experiences large seasonal temperature variations, as it is positioned in a zone of significant equatorial upwelling, a result of strong trade winds and the Equatorial Undercurrent (EUC) shoaling as it meets the western coast of Isabela Island during the boreal summer months (Kessler, 2006; Trueman and d'Ozouville 2010; Conroy et al., 2014). Our new records originate from Genovesa Island (0.32°N, 89.96°W), in the northeastern part of the archipelago, where SST ranges seasonally from 26.8°C (March) to 23.1°C (August). El Niño events are strongly imprinted as warm SST anomalies, as upwelling weakens or disappears (Conroy et al., 2014). Warm SSTAs in the Galapagos are a reliable indicator of ENSO anomalies.

Wolf and Darwin Islands lie in the northwestern section of the Galápagos archipelago, approximately 150 km and 180 km from the central platform, respectively. Being more distant from the primary upwelling zone of the Galápagos, these regions experience less SST variability than do the other sites (Sweet et al., 2007). Wolf experiences a seasonal temperature range

between 23.9-27.1°C, and Darwin SST ranges from 24.6-27.4°C, more typical of tropical oceans than the rest of the archipelago. The coolest of our Galápagos sites, Urvina Bay, lies on the west coast of Isabela Island, at the site of a former reef that was tectonically uplifted in the 1950's CE, as described in Dunbar et al. (1994). This site experiences the strongest SST seasonality in Galápagos, ranging from 20.8 to 26.0°C.

New $\delta^{18}\text{O}$ Records from Genovesa Island

This study presents new $\delta^{18}\text{O}$ data from two cores collected in 2016 from Genovesa Island. The cores, GEN-16-1 and GEN-16-3, were drilled in two subfossil *Porites lobata* corals found along the shoreline of Darwin Bay, using a hand-held gasoline powered rock drill with a 10 cm core bit, cooled by seawater.

The cores were imaged using a computed tomography (CT) scanner before slabbing to identify the best axis of vertical growth (Fig. S1). CT images provide a 3-dimensional view of coral growth direction and a more comprehensive view of coral growth features than traditional 2-dimensional x-rays (Cantin and Lough, 2014; DeCarlo et al., 2015). Once slabbed, the corals were sampled at 1-mm resolution along their optimum growth axis (DeLong et al., 2012) using a computer-controlled micromill. The computer allowed for precise depth and width measurements of each transect. Drilling produced a powder sample representing ~1 month. We weighed 30-60 μg samples for stable isotopic analysis using a Delta +/Kiel IV carbonate mass spectrometer in the Paleoclimate and Common Era lab at the University of Michigan. To rule out post-depositional alteration, typically seen as aragonite overgrowths on the coral skeleton, we

imaged several spots on both cores using scanning electron microscopy (SEM). We found no evidence of secondary aragonite in either core (Fig. S2).

Reprocessing Published Coral Paleorecords

To supplement our records and place them in context, published coral paleorecords from the Galápagos (EP) and the Northern Line Islands (CP) were included this study. All coral records used in this study are summarized in Table S1A (EP) and S1B (CP). Some of the pre-published coral records were reprocessed due to age uncertainties and problematic sampling transects. For the fossil Wolf 10-04 core, we resampled 2 transects identified by Reed et al. (2021) as being problematic (CT1 and CT2) and analyzed these samples for Sr/Ca. We find that transect CT1 overlaps well with the newly resampled data, and that there is a small offset (and more apparent noise) in CT-2 compared to the newly sampled data. This observation suggests an earlier analysis of transect quality (Reed et al. 2021) may have been overly critical in terms of how it reflects on data quality. For other suboptimal transects, we removed data from suboptimal transect G1 (thereby truncating the record by a few years), and we retained data from D2A. On slab D, the transect quality was reassessed in part as being acceptable, and where it displayed potential problems, we found no better alternate transect. The data derived from the new transects were age modeled as in Reed et al. (2021).

We redated the Urvina Bay coral record, because the original data (Druffel et al. 2015) were unevenly spaced in time and had not been assigned ages according to geochemical seasonality, making removal of the seasonal cycle difficult. To be consistent with our other records, we redated this record by aligning the warmest month of the year (March) with the most

depleted $\delta^{18}\text{O}$ value (see “Data Processing”). We note the seasonal cycle in this record is less consistent than in other cores, potentially reflecting either 1) irregular growth in this thermally challenging environment; 2) microsampling that did not account for species-specific growth considerations in this seldom-used taxon; or 3) the sub-horizontal orientation of the drill core (Dunbar et al. 1994). This record originated from a *Pavona clavus* colony, unlike the other three fossil EP corals from *Porites lobata*. In the central Pacific, we opted to analyze individual coral records from the northern Line Islands, rather than the spliced 17th-century record presented in Cobb et al. (2003; 2013).

20th Century Coral Records

We included several published 20th-21st century coral records to compare with 17th-18th century coral records (we include these in our “20th-century” designation; see “Defining Intervals for Comparison”). EP 20th century records include a $\delta^{18}\text{O}$ record from Darwin Island (Jimenez, 2019) that is divided into two individual records: one before (GD15 3-2a) and one after (GD15 3-2b) the 1983 El Niño death horizon. This study also includes a Sr/Ca record from Darwin Island, GD15 3-1 (Cheung et al., unpublished). Also included are two Sr/Ca records from Wolf Island (Jimenez et al., 2018), with the Wolf 10-03 core divided into two records (Wolf 10-03a and Wolf 10-03b) at the 1983 death horizon. All EP 20th century coral records used in this study are summarized in Table S1A.

The CP 20th century coral records used in this study are all $\delta^{18}\text{O}$, including three Christmas Island records (Evans et al., 1999; Grothe et al., 2019; Nurhati et al., 2009), three Palmyra Island records (Cobb et al., 2001; Nurhati et al., 2009; Sanchez et al., 2020), and four

Fanning Island records (Nurhati et al., 2009; Cobb et al., 2013; Sanchez et al., 2020). To determine “recent modern variability,” spliced records from Palmyra (Sanchez et al., 2020) and Christmas Island (Grothe et al., 2019) were utilized (See “Defining Intervals for Comparison”). All CP 20th century coral records used in this study are summarized in Table S1B.

DATA PROCESSING

First, raw $\delta^{18}\text{O}$ and Sr/Ca values were interpolated to monthly values by assigning the most depleted values with the warmest month at each location. We used seasonal variations in skeletal $\delta^{18}\text{O}$ to identify years within each core, by lining up the most depleted $\delta^{18}\text{O}$ values with the warmest month at each location. For example, Genovesa Island experiences its warmest SSTs during February, so the most depleted $\delta^{18}\text{O}$ values were assigned to be the second month of the year. Then, the raw data were interpolated using Acycle, a MATLAB-based analysis program, to monthly resolution (Li et al., 2019). In the case of our two new coral records, ages were assigned to the coral based on U/Th dates provided by the University of Minnesota (Edwards et al., 1987), and seasonal $\delta^{18}\text{O}$ cycles provided internal annual age assignments. Next, we removed the seasonal cycle from the records by subtracting the average monthly SST value from each month, yielding records of SSTAs for subsequent analysis.

To enable direct comparison of all coral records, we converted $\delta^{18}\text{O}$ and Sr/Ca data to SST. $\delta^{18}\text{O}$ values undergo temperature-dependent fractionation at approximately $-0.2\text{‰ } \delta^{18}\text{O}/^{\circ}\text{C}$ (Epstein et al., 1953; McConnaughey et al., 1989; Wellington et al. 1996), so this conversion was

used for all of the $\delta^{18}\text{O}$ records unless otherwise specified by an author (see Table S2). Sr/Ca anomalies were converted based on published calibrations (Table S2). Lastly, all SSTA records from Wolf or Darwin Island were scaled by a factor of 1.2 to match the variability experienced at other locations in the Galápagos. HadiSST data from these islands revealed naturally higher variability at Genovesa and Urvina Bay (Rayner et al., 2003), and were used to derive this calibration value.

We processed the reconstructed monthly SST anomalies in two distinct ways, to compare two methods of quantifying ENSO variance that have emerged in the literature. In the first method, we used a 2-7-year bandpass filter to isolate the time scale of ENSO, and then computed the standard deviation (following Tudhope et al., 2001; Cobb et al., 2003; 2013). However, a 2-7-year bandpass filter is not optimal for short (<30 year) datasets, because it effectively reduces dataset length. In the second approach, we applied a 9 year-high-pass filter to remove decadal and longer variability, smoothed the data with a 5-month running mean (6 month for bi-monthly sampled data), and calculated the probability density function (PDF), using a kernel density estimation method (Parzen, 1962; after Lawman et al. 2020). The PDF method is more effective on shorter datasets because it considers the distribution of all of the data without loss (Trenberth, 1997; Lawman et al., 2020). More importantly, from the PDF, we can evaluate the occurrence of extreme ENSO events – a separate measure of ENSO variability and arguably more impactful than variance, from a societal perspective (Trenberth, 1997). We identify extreme events as those occurring outside the 2.5% and 97.5% distribution ($p_{2.5}$ and $p_{97.5}$) and calculated the spread of each dataset between $p_{2.5}$ and $p_{97.5}$ as a measure of variability for comparison among and between sites and time intervals. We performed this analysis on the entire length of each record, and on

20-yr segments, stepped by 1 year, for each record, to identify where longer records contained epochs of higher and lower variance (Fig S3).

Defining Intervals for Comparison

It has been proposed that the most significant ENSO intensification has occurred mainly in the last two decades, relative to the last several hundred years, and even to the last century (e.g., Cobb et al., 2003; 2013; Freund et al., 2019; Grothe et al., 2019; Sanchez et al., 2020). It is therefore difficult to determine recent intensification of ENSO by comparing published 17th-18th century coral records (hereafter referred to as “fossil” records), to currently published 20th century records, which can include data that extend back throughout the 1800’s and early 1900’s. Therefore, we define a new interval, the “recent modern” interval, by extracting SSTA variability from the 1990-2010 CE window from 20th-21st century records that are currently available. This results in three distinct intervals that can be used for comparison: a “fossil” interval, that includes SSTA data spanning ~1670-1830 CE, a “20th century” interval, spanning ~1860-2015 CE (variable among sites), and a “recent modern” interval, limited to 1990-2010 CE. Since 21st century coral data remains sparse, particularly in the CP, spliced coral records from Christmas (Grothe et al., 2019) and Palmyra Island (Sanchez et al., 2020) were used to evaluate the recent modern interval in the CP, but we did not use splices to assess the 20th century. Finally, one of the EP coral records (GD15 3-2b) only extended back to 1991 CE, so the 1991-2010 CE window was used to define the recent modern interval for this record only.

RESULTS

New/Reprocessed Fossil EP Age Dates and Record Lengths

The four EP fossil interval coral records in this study are either new, resampled, or reprocessed since their original publication. Their ages, length, and proxy type are summarized below and in Fig. 3 and Table S1A. The new fossil GEN-16-1 and GEN-16-3 cores date to CE 1678 (± 2 yr) and 1758 (± 1 yr). The cores span 32 and 23 years, respectively, covering the intervals of 1678-1710 CE and 1758-1781 CE. Once the problematic transects were resampled, the fossil Wolf 10-04 core from Reed et al (2021) dates to CE 1693, covering 83 years (1693-1776 CE). After reprocessing, the fossil Urvina Bay UR-86 core from Druffel et al. (2015) dates to CE 1783, spanning 52 years (1783-1835 CE).

Bandpass Filtering/Standard Deviation Method

Recent modern variability, represented by the horizontal dashed line at 0 in Figures 4A and 4B, is defined as the standard deviation of the 2-7 year bandpass-filtered 20th century coral SSTA values spanning 1990-2010 CE. In the EP, we used the average from the Darwin GD15 3-1 (Cheung et al., unpublished) and GD15 3-2 (Jimenez, 2019) records, as well as the Wolf 10-10 and 10-03 records (Jimenez et al., 2018) (Fig. 4A). In the CP, we defined the modern variability as above using the Palmyra (Sanchez et al., 2020) and Christmas (Grothe et al., 2019) spliced records, as well as an independent Christmas Island record, X12-6 (Grothe et al., 2019; Fig. 4B). Each dot on the graph reflects the percentage difference between that record's standard deviation

(variability) and that of the recent modern interval. Dots that plot above the dashed line represent stronger ENSO variance than the recent modern, and those below, weaker. The positive and negative vertical error bars on each dot represent the maximum and minimum standard deviation values of each record, quantified by calculating the standard deviation of 20-yr moving intervals (incremented at 1-month time steps). Vertical bars thus show the full range of variability that each record displayed during their respective time windows. Records from each interval are shaded with a different color box to highlight differences in variability.

In the EP, we find a slight increase in variability in the 20th century interval compared to the fossil interval, and a substantial increase in the recent modern interval compared to the fossil interval (Fig. 4A). This represents an increase in EP ENSO variance since the early 19th century, with the most intense increase in the last two decades. We find no overlap between the variability of the recent modern interval and that of the fossil interval. In the CP, however, the 20th century and recent modern intervals show little increase in variance over the fossil interval (Fig 4B). Unlike the EP data, variance in the three intervals overlaps substantially. CP fossil interval variance is more comparable to 20th century and recent modern variance than in the EP, signaling a greater increase in variance in the modern EP than in the CP.

High-pass/PDF Method

The EP fossil interval PDF curves are narrower than the EP 20th century and recent modern interval curves (Fig. 5A), signaling less variance during the fossil interval than the 20th century and recent modern. This result is consistent with the standard deviation/bandpass method results. The average spread of the fossil interval curves is 2.94, compared to a 20th century

average of 4.83. The average spread of the recent modern interval curves is the highest, with a value of 4.99 (Fig. 6A; Table S3A-B). The lower average spread value in the fossil records represents weaker ENSO activity during the fossil interval than during the 20th century interval, whereas the recent modern interval is much more variable than both earlier intervals.

CP fossil PDF spreads were more similar to 20th century and modern spreads than in the EP, although a slight increase in variance can be observed since the fossil interval (Fig. 5B). This result is also consistent with the standard deviation/bandpass results. The average spread of the CP fossil PDF curves is 2.17, the 20th century is 2.86, and the recent modern is the highest at 3.03 (Fig. 6B; Table S3C-D). However, the spread for individual cores overlaps among these intervals. This result reveals that in the CP, ENSO variability has increased mildly, if at all, since the fossil interval.

DISCUSSION

EP ENSO Variability

In the EP, we find a pattern of increasing variance from the fossil interval, through the 20th century, into the recent modern. We find a clear increase in variance between the fossil interval and the 20th century (Fig. 4A). By contrast, the recent modern interval displays far higher standard deviation values; the range of variance does not overlap with the fossil interval. These results are echoed in the EP PDF curves. The 20th century curves are distinctly wider than the fossil curves (Fig. 5A; Fig. 6A), and the recent modern interval produces even wider curves.

Moreover, these results almost certainly underestimate the true modern variance, because none of the modern Galápagos corals grew during the strong 1982-3 and 2015-16 events (our recent modern interval includes only one of the three largest recent events, that in 1997-8). Our results suggest that ENSO activity in the eastern Pacific has been intensifying since the pre-industrial era, with the most significant increase occurring in the most recent modern era (1990-2010 CE).

CP ENSO Variability

In the CP, 20th century variance encompasses the full range of variability seen in both the fossil and the recent modern, and there is less of a discernable trend than in the EP (Fig. 4B). The fossil and recent modern interval data overlap substantially, although we note that three of the four fossil CP records have distinctly lower variance compared to the 20th century records. This result is consistent when evaluating the recent modern, 20th century, and fossil PDF curves, which have comparable spread widths (Fig. 5B; Fig. 6B). Our CP results suggest that recent modern ENSO variance doesn't appear to be substantially higher than 20th century variance. While variance in the recent modern interval is the highest of the intervals evaluated in this study, our results suggest that this higher variance is not unique to the last 50 years, in agreement with Cobb et al. (2013). Our results are not at odds with CP studies that demonstrate anomalously high ENSO variance in the most recent decades, relative to previous millennia (Grothe et al., 2019). However, our data focus on the last 400 years, a time in which CP variance appears to have changed little. Our analysis uses individual coral records, not spliced records, to assess past variability. We find that the 20th century CP variance is large and encompasses the range of variability in both fossil and recent modern intervals.

Variance change in the EP records remains more distinct and abrupt than in the CP, almost doubling since pre-industrial levels. Below, we consider the possible mechanisms for a substantial increase in modern EP El Niño variability. We also compare our results to other EP and tropical Pacific paleoclimate data, and we evaluate our results in the context of ENSO's response to anthropogenic greenhouse forcing.

Other EP and Tropical Pacific Paleoclimate Data

Comparisons between other EP paleoclimate records that evaluate the last few decades and can precisely separate them from the fossil interval investigated in this study are limited, because we lack ENSO-sensitive coral records from this region that cover both the 17th-18th century and the last few decades. Here, we compare our reconstructions with other studies that broadly address changes in mean and variance over the past 500 years.

Sediment cores from El Junco Lake on San Cristobal Island, Galápagos, suggest a strong increase in ENSO activity between the fossil interval investigated in this study and the 20th century. El Junco hydrology is sensitive to changes in precipitation, with lake levels rising up to 6 meters during intervals of heavy rain (Conroy et al., 2008). Based on lake diatom assemblages that track lake level, these authors infer high rainfall and suggest that regional SST in the last 50 years is the highest in their 1200-year record (Conroy et al., 2009). These results support increasing frequency of strong El Niño events, which bring high rainfall amounts. However, Wolff (2010) argues that regional SST has not displayed the substantial 20th-century warming inferred by Conroy et al. (2008). Subsequent coral work has indicated a more subdued warming since the mid-20th century (Jimenez et al. 2018); these data comprise part of our analysis here.

Single-foraminifera analysis from marine sediments suggest that EP ENSO variability was relatively high, but variable, during the fossil interval investigated in this study (Rustic et al., 2015). Comparing these results to ours presents challenges: precise chronological synchronization is difficult given the radiocarbon-based age model of the sediment records, and the single-foraminifera approach has been argued to be more sensitive to the seasonal cycle than ENSO in the surface waters of the EP (Thirumalai et al., 2013).

Using a Pacific-wide network of coral records, Freund et al. (2019) found a significant increase in variability in the EP cold tongue during the 20th century. They suggest that although EP events are not increasing in frequency in the modern interval, relative to CP events, they are becoming more intense. Other multi-site coral networks, along with multiproxy indices of ENSO (e.g., McGregor et al. 2008; Braganza et al., 2009; Emile-Geay et al. 2013), show enhanced variability in the 20th century compared to earlier intervals, but these studies do not distinguish CP vs. EP events. We note that in multi-site reconstructions, increases in 20th century variance may be artificial, resulting from age model biases and inhomogeneous data (e.g., greater coverage of the equatorial Pacific after ~1890; Comboul et al. 2014; Loope et al. 2020).

Is EP ENSO Intensification a Response to Anthropogenic Greenhouse Forcing?

Using observations since CE 1901, Wang et al. (2019) identify trends in the recurrence of 4 distinct ENSO types and describe the conditions that lead to their onset and amplification. They find that strong basin-wide (SBW) events are intensifying, driven by a stronger zonal SST gradient. This enhanced gradient is due to disproportionate heating of the western Pacific (WP), which these authors attribute at least partly to global warming. They note that these SBW events

have increased significantly in frequency since the late 1970's, when substantial WP warming began, and that these events cause a high degree of variability in the EP (and dramatic climate impacts beyond the Pacific). Over the course of the 20th century, moderate CP (MCP) events have also become more common, whereas moderate EP (MEP) events have become less frequent. These results agree with our analysis that EP variance is intensifying and provide the context to link our observations with an increasing SST gradient across the equatorial Pacific.

Our results are also consistent with a recent coupled model study that finds intensified EP event strength as anthropogenic warming proceeds through the 21st century (Cai et al. 2018). Using a subset of CMIP5 models that simulate distinct EP and CP regimes, these authors found that EP El Niño events increased in amplitude under radiative forcing (RCP8.5 scenario) by an average of 15%. They attribute this increase largely to two factors: enhanced warming in the equatorial Pacific (Xie et al. 2008), and more importantly, increased vertical stratification across the equatorial Pacific resulting from surface warming everywhere. This stratification strengthens ocean-air coupling, resulting in stronger positive ENSO feedbacks as anomalies develop.

More generally, the question of ENSO's potential response to anthropogenic greenhouse forcing remains actively debated; two general responses have received wide attention. In the "Ocean Dynamical Thermostat" (ODT) model proposed by Clement et al. (1996), uniform warming across the Pacific leads to a stronger zonal SST gradient and a steeper equatorial thermocline: upwelling maintains cool EP SST while the WP warms, strengthening the zonal SST gradient and intensifying the Walker circulation. This creates a positive feedback loop that continues to enhance trade wind strength, the SST gradient, and upwelling in the EP (Luo et al.,

2017; Cai et al., 2018). The warming and increased gradient described by Wang et al. (2019), which support the increased frequency of strong basin-wide events, appears to agree with this general response. By contrast, the “Weakened Walker” hypothesis suggests that the Walker circulation over the tropical Pacific will diminish in response to anthropogenic forcing, as a result of the imbalance between the global atmospheric water vapor increase and the rate of precipitation (Vecchi and Soden, 2007). In this scenario, the zonal SST gradient would decrease, weakening trade winds and creating a flatter thermocline. Most CMIP5 models project this response (DiNezio et al. 2013; Kociuba and Power 2015; Plesca et al. 2018; Coats and Karnauskas 2017), although some models show no change, or even a strengthening of the Walker circulation with continued forcing (e.g., Kohyama et al. 2017).

Recent studies suggest that the ODT response may be an initial, but short-lived, response to radiative forcing that gives way to an equilibrium response resembling the weaker Walker scenario (Kim et al., 2014; Luo et al., 2017; Heede et al., 2020). Important contributors to this transition include the overturning subtropical cells that bring increasingly warm water from the surface subtropics into the equatorial thermocline over periods of decades (Luo et al., 2017; Heede et al., 2020). In this interpretation, the “tug of war” between these mechanisms will determine the path of ENSO variance over the coming century (Heede et al 2020).

The implications for variability under these two mechanisms are unclear: on one hand, the flatter thermocline and reduced SST gradient of the weaker Walker scenario imply El Niño like conditions, which tend to exhibit higher variance. On the other hand, very strong basin-wide events require preconditioning with the accumulation of large volume of warm water in the WP,

which would occur under a stronger SST gradient and steeper thermocline – the ODT scenario – as described by Wang et al. (2019). Overall, our coral data are consistent with the arguments put forth by Wang et al. (2019) and Cai et al. (2018) that increasing radiative forcing will lead to intensifying ENSO variability in the eastern Pacific. A more extensive preindustrial dataset from this region is needed to confirm the bounds of preindustrial variance and the transient response of EP variability to radiative forcing.

CONCLUSIONS

Climate observations from the equatorial Pacific are notably sparse, and combined with the large internal variability in this region, identifying long-term trends in ENSO has proven a difficult challenge. Here we present new and updated coral records from the Galápagos islands that add to our understanding of past ENSO variability in an under-sampled yet critical part of the tropical Pacific. Based on new and reanalyzed coral data from the Galápagos, we have identified a signal of intensifying eastern Pacific ENSO variability during the 20th century, with the most significant increase occurring during the recent modern interval of 1990-2010 CE. Comparison with previously published ENSO variability records from the central Pacific reveal a less substantial increase in variance, with comparable fossil, 20th century, and recent modern ENSO variability in accordance with Cobb et al. (2013). This suggests that since the 17th-18th centuries, ENSO variability is increasing primarily in the EP, with CP variance that is not unique to the recent modern interval. Increased modern EP variance may be a result of anomalously strong basin-wide events that share the characteristics of both moderate and very strong EP

events, which have become significantly more common since ~1970 (Wang et al., 2019). Projections from coupled climate models, in particular a subset of CMIP5 simulations, further support the strengthening of future EP ENSO events, a consequence of increased vertical stratification of SSTs in the eastern Pacific as warming continues (Cai et al., 2018).

Our results align with these disturbing projections of greater ENSO variance in a warmer world and imply growing dangers for human and natural systems. Stronger SST variance adds new extremes to anthropogenic warming and threatens thermally sensitive coral reefs and other ecosystems. Stronger SST variance also amplifies local and remote impacts on hydroclimate – which may already be intensifying simply by occurring in a warmer atmosphere (Power et al., 2017). Although the details of the physical processes underlying increasing ENSO variance have yet to be fully reflected in current climate model projections, we argue that coral records such as these provide expanding evidence for systematic changes in ENSO that are compounding the planetary risks of continued anthropogenic climate change.

BIBLIOGRAPHY

- Abram, N.J., Wright, N.M., Ellis, B., Dixon, B.C., Wurtzel, J.B., England, M.H., Ummenhofer, C.C., Philibosian, B., Cahyarini, S.Y., Yu, T-L., Shen, C-C., Cheng, H., Edwards, R.L., and Heslop, D., 2020, Coupling of Indo-Pacific climate variability over the last millennium: *Nature*, v.579, p.385-407. doi.org/10.1038/s41586-020-2084-4
- Ashok, K., Behera, S.K., Rao, S.A., Weng, H., and Yamagata, T., 2007, El Niño Modoki and its possible teleconnection: *Journal of Geophysical Research*, v.112, p.1-27. doi.10.1029/2006JC003798
- Barrett, H.G., Jones, J.M., and Bigg, G.R., 2016, Reconstructing El Niño Southern Oscillation using data from ships' logbooks, 1815–1854. Part I: methodology and evaluation: *Climate Dynamics*, v.50, p.845-862. doi.10.1007/s00382-017-3644-7
- Beck, J.W., Edwards, R.L., Ito, E., Taylor, F.W., Recy, J., Rougerie, F., Joannot, P., and Henin, C., 1992, Sea-Surface Temperature from Coral Skeletal Strontium/Calcium Ratios: *Science*, v.257, p.644-647. doi.10.1126/science.257.5070.644.
- Bjerknes, J., 1969, Atmospheric teleconnections from the equatorial Pacific: *Monthly Weather Review*, v.97, p.163–172. doi.10.1175/1520-0493(1969)097<0163:ATFTEP>2.3.CO;2
- Braganza, K., Gergis, J.L., Power, S.B., Ribsey, J.S., and Fowler, A.M., 2009, A multiproxy index of the El Niño–Southern Oscillation, A.D. 1525–1982: *Journal of Geophysical Research*, v.114, p.1-17. doi.10.1029/2008JD010896
- Cai, W., Borlace, S., Lengaigne, M., van Rensch, P., Collins, M., Vecchi, G., Timmermann, A., Santoso, M., McPhaden, M.J., Wu, L., England, M.H., Wang, G., Guilyardi, E., and Jin, F.-F., 2014, Increasing frequency of extreme El Niño events due to greenhouse warming: *Nature Climate Change*, v.4, p.111–116. doi.10.1038/nclimate2100
- Cai, W., Wang, G., Dewitte, B., Wu, L., Santoso, A., Takahashi, K., Yang, Y., Carréric, A., and McPhaden, M.J., 2018, Increased variability of eastern Pacific El Niño under greenhouse warming: *Nature*, v.564, p.201–206. doi.10.1038/s41586-018-0776-9
- Cai, W., Wang, G., Santoso, A., McPhaden, M. J., Wu, L., Jin, F.-F., Timmermann, A., Collins, M., Vecchi, G., Lengaigne, M., England, M.H., Dommenges, D., Takahashi, K., and Guilyardi, E., 2015, More frequent extreme La Niña events under greenhouse warming: *Nature Climate Change*, v.5, p.132–137. doi.org/10.1038/nclimate2492
- Cantin N.E., and Lough, J.M., 2014, Surviving Coral Bleaching Events: Porites Growth Anomalies on the Great Barrier Reef: *Public Library of Science One*, v.9, p.1-12. doi.10.1371/journal.pone.0088720
- Capotondi, A., 2013, ENSO diversity in the NCAR CCSM4: *Journal of Geophysical Research*, v.118, p.4755–4770. doi.10.1002/jgrc.20335
- Capotondi, A., and Sardeshmukh, P.D., 2015, Optimal precursors of different types of ENSO events: *Geophysical Research Letters*, v.42, p.9952–9960. doi.10.1002/2015GL066171
- Capotondi, A., Wittenberg, A.T., Kug, J.-S., Takahashi, K., and McPhaden, M.J., 2021, ENSO Diversity, *in* McPhaden, M.J., Santoso, A., and Cai, W., ed. 1, *El Niño Southern Oscillation in a Changing Climate*, *Geophysical Monograph* 253: John Wiley & Sons, Inc., p.65-86.
- Cheung, A.H., Cole, J.E., Thompson, D.M., Vetter, L., Reed, E.V., Jimenez, G., and Tudhope, A.W., *in preparation for Paleoceanography and Paleoclimatology*
- Clement, A.C., Seager, R., Cane, M.A., and Zebiak, S., 1996, An Ocean Dynamical Thermostat: *Journal of Climate*, v.9, p.2190-2196. doi.10.1175/1520-0442(1996)009<2190:AODT>2.0.CO;2

- Coats, S., and Karnauskas, K.B., 2017, Are Simulated and Observed Twentieth Century Tropical Pacific Sea Surface Temperature Trends Significant Relative to Internal Variability?: *Geophysical Research Letters*, v.44, p.9928-9937. doi.org/10.1002/2017GL074622
- Cobb, K.M., Charles, C.D., Cheng, H., and Edwards, R.L., 2003, El Niño/Southern Oscillation and tropical Pacific climate during the last millennium: *Nature*, v.424, p.271-276. doi.org/10.1038/nature01779
- Cobb, K.M., Charles, C.D., and Hunter, D.E., 2001, A central tropical Pacific coral demonstrates Pacific, Indian, and Atlantic decadal climate connections: *Geophysical Research Letters*, v.28, p.2209-2212. doi.org/10.1029/2001GL012919
- Cobb, K.M., Westphal, N., Sayani, H.R., Watson, J.T., Di Lorenzo, E., Cheng, H., Edwards, R.L., and Charles, C.D., 2013, Highly Variable El Niño-Southern Oscillation Throughout the Holocene: *Science*, v. 339, p. 67-70. doi.10.1126/science.1228246
- Cole, J.E., J.T. Overpeck, and E.R. Cook, 2002, Multiyear La Niña events and persistent droughts in the contiguous United States: *Geophysical Research Letters*, v.29. doi.10.1029/2001GL013561
- Cole, J.E. and Tudhope, A.W. 2017, Reef-based reconstructions of eastern Pacific climate variability. *in* Glynn PW, Manzello D, Coral Reefs of the Eastern Pacific: Persistence and Loss in a Dynamic Environment, Springer Netherlands. doi.10.1007/978-94-017-7499-4_19
- Comboul, M., Emile-Geay, J., Evans, M.N., and Mirnateghi, N., 2013, A probabilistic model of chronological errors in layer-counted climate proxies: applications to annually-banded coral archives: *Climate of the Past Discussions*, v.9, p. 6077-6123. doi.10.5194/cpd-9-6077-2013
- Conroy, J.L., Overpeck, J.T., Cole, J.E., Shanahan, T.M., and Steinitz-Kannan, M., 2008, Holocene changes in eastern tropical Pacific climate inferred from a Galápagos lake sediment record: *Quaternary Science Reviews*, v.27, p.1166-1180. doi.10.1016/j.quascirev.2008.02.015
- Conroy, J.L., Restrepo, A., Overpeck, J.T., Steinitz-Kannan, M., Cole, J.E., Bush, M.B., and Colinvaux, P.A., 2009, Unprecedented recent warming of surface temperatures in the eastern tropical Pacific Ocean: *Nature Geoscience*, v.2, p.46-50. doi.10.1038/NGEO390
- Conroy, J.L., Thompson, D.M., Collins, A., Overpeck, J.T., Bush, M.B., and Cole, J.E., 2014, Climate influences on water and sediment properties of Genovesa Crater Lake, Galápagos: *Journal of Paleolimnology*, v.52, p.331-347. doi.10.1007/s10933-014-9797-z
- Conroy, J.L., Thompson, D.M., Cobb, K.M., Noone, D., Rea, S., and Legrande, A.N., 2017, Spatiotemporal variability in the $\delta^{18}\text{O}$ -salinity relationship of seawater across the tropical Pacific Ocean: *Paleoceanography*, v.32, p.484-497. doi.org/10.1002/2016PA003073
- DeCarlo, T. M., Gaetani, G. A., Holcomb, M., and Cohen, A. L., 2015, Experimental determination of factors controlling U/Ca of aragonite precipitated from seawater: Implications for interpreting coral skeleton: *Geochimica et Cosmochimica Acta*, v. 162, p. 151–165. doi. org/10.1016/j.gca.2015.04.016
- Delong, K.L., Quinn, T.M., Taylor, F.W., Shen, C.-C., and Lin, K., 2012, Improving coral-base paleoclimate reconstructions by replicating 350 years of coral Sr/Ca variations: *Paleogeography, Paleoclimatology, Paleoecology*, p.1-19. doi.org/10.1016/j.palaeo.2012.08.019
- Deser, C., Alexander, M.A., Xie, S.-S., and Phillips, A.S., 2010, Sea Surface Temperature Variability: Patterns and Mechanisms: *The Annual Review of Marine Science*, v.2, p.115-143. doi.10.1146/annurev-marine-120408-151453
- DiNezio, P.N., and Tierney, J.E., 2013, The effect of sea level on glacial Indo-Pacific climate: *Nature Geoscience*, v.6, p.485-491. doi.org/10.1038/ngeo1823

- Druffel, E.R.M., Griffin, S., Vetter, D., Dunbar, R.B., and Mucciarone, D.M., 2015, Identification of frequent La Niña events during the early 1800s in the east equatorial Pacific: *Geophysical Research Letters*, v.42, p.1512-1519. doi.10.1002/2014GL062997
- Dunbar, R.B., Wellington, G.M., Colgan, M.W., and Glynn, P.W., 1994, Eastern Pacific sea surface temperature since 1600 A.D.: The $\delta^{18}\text{O}$ record of climate variability in Galápagos Corals: *Paleoceanography*, v.9, p.291-315. doi.10.1029/93PA03501
- Edwards, R.L., Chen, J.H., and Wasserburg, G.J., 1987, ^{238}U - ^{234}U - ^{230}Th - ^{232}Th systematics and the precise measurement of time over the past 500,000 years: *Earth and Planetary Science Letters*, v.81, p.175-192. doi.org/10.1016/0012-821X(87)90154-3
- Emile-Geay, J., Cobb, K.M., Carré, M., Braconnot, P., Leloup, J., Zhou, Y., Harrison, S.P., Corrège, T., McGregor, H.V., Collins, M., Driscoll, R., Elliot, M., Schneider, B., and Tudhope, A., 2016, Links between tropical Pacific seasonal, interannual and orbital variability during the Holocene: *Nature Geoscience*, v.9, p.168-175. doi.10.1038/NGEO2608
- Emile-Geay, J., Cobb, K.M., Cole, J.E., Elliot, M., and Zhu, F., 2021, Past ENSO Variability: Reconstructions, Models, and Implications, *in* McPhaden, M.J., Santoso, A., and Cai, W., ed. 1, *El Niño Southern Oscillation in a Changing Climate*, Geophysical Monograph 253: John Wiley & Sons, Inc., p.87-118.
- Emile-Geay, J., Cobb, K.M., Mann, M.E., and Wittenberg, A.T., 2013, Estimating Central Equatorial Pacific SST Variability over the Past Millennium. Part II: Reconstructions and Implications: *American Meteorological Society*, v. 26, p.2329-2352. doi.org/10.1175/JCLI-D-11-00511.1
- Epstein, S., Buchsbaum, R., Lowenstam, H.A., and Urey, H.C., 1953, Revised Carbonate-Water Isotopic Temperature Scale: *Bulletin of the Geological Society of America*, v.64, p.1315-1326.
- Evans, M.N., Fairbanks, R.G., and Rubenstone, J.L., 1999, The thermal oceanographic signal of El Niño reconstructed from a Kiritimati Island coral: *Journal of Geophysical Research: Oceans*, v.104, p.13409-13421. doi.org/10.1029/1999JC900001
- Freund, M.B., Henley, B.J., Karoly, D.J., McGregor, H.V., Abram, N.J., and Dommenges, D., 2019, Higher frequency of Central Pacific El Niño events in recent decades relative to past centuries: *Nature Geoscience*, v.12, p.450-455. doi.org/10.1038/s41561-019-0353-3
- Glynn, P.W., Manzello D.P., 2015, Bioerosion and Coral Reef Growth: A Dynamic Balance, *in* Birkeland C. (eds) *Coral Reefs in the Anthropocene*: Springer, Dordrecht, p.67-97. doi.org/10.1007/978-94-017-7249-5_4
- Glynn, P.W., Riegl, B., Correa, A.M.S., and Baums, I.B., 2009, Rapid Recovery of a Coral Reef at Darwin Island, Galapagos Islands: *Galapagos Research*, v.6, p.6-13. doi.https://nsuworks.nova.edu/occ_facarticles/347.
- Goddard, L., and Dilley, M., 2005, El Niño: Catastrophe or opportunity: *Journal of Climate*, v.18, p. 651–665. doi.org/10.1175/JCLI-3277.1
- Goddard, L., and Gershunov, A., 2021, Impact of El Niño on Weather and Climate Extremes, *in* McPhaden, M.J., Santoso, A., and Cai, W., ed. 1, *El Niño Southern Oscillation in a Changing Climate*, Geophysical Monograph 253: John Wiley & Sons, Inc., p.3-19.
- Grothe, P.R., Cobb, K.M., Liguori, G., Di Lorenzo, E., Capotondi, A., Lu, Y., Cheng, H., Edwards, R.L., Southon, J.R., Santos, G.M., Deocampo, D.M., Lynch-Stieglitz, Chen, T., Sayani, H.R., Thompson, D.M., Conroy, J.L., Moore, A.L., Townsend, K., Hagos, M., O'Connor, G., and Toth, L.T., 2019, Enhanced El Niño-Southern Oscillation Variability in Recent Decades: *Geophysical Research Letters*, v.47, p.1-8. doi.10.1029/2019GL083906

- Heede, U.K., Fedorov, A.V., and Burls, N.J., 2020, Time Scales and Mechanisms for the Tropical Pacific Response to Global Warming: A Tug of War between the Ocean Thermostat and Weaker Walker: *American Meteorological Society*, v.33, p.6101-6118. doi.10.1175/JCLI-D-19-0690.1
- Jimenez, G., Cole, J.E., Thompson, D.M., and Tudhope, A.W., 2018, Northern Galápagos Corals Reveal Twentieth Century Warming in the Eastern Tropical Pacific: *Geophysical Research Letters*, v.45, p.1-8. doi.10.1002/2017GL075323
- Jimenez, G., 2019, *Reconstructing Tropical Pacific Climate Variability from Coral Archives*, 134 p, University of Arizona, Tucson, AZ.
- Kao, H.-Y., and Yu, J.-Y., 2009, Contrasting Eastern-Pacific and Central-Pacific Types of ENSO: *American Meteorological Society*, v.22, p.615-632. doi.10.1175/2008JCLI2309.1
- Kessler, W.S., 2006, The circulation of the eastern tropical Pacific: A review: *Progress in Oceanography*, v.69, p.181-217. doi.org/ 10.1016/j.pocean.2006.03.009
- Kim, S.T., Cai, W., Jin, F.-F., and Yu, J.Y., 2014, ENSO stability in coupled climate models and its association with mean state: *Climate Dynamics*, v.42, p.3313-3321. doi.org/10.1007/s00382-013-1833-6
- Kociuba, G., and Power, S.B., 2015, Inability of CMIP5 Models to Simulate Recent Strengthening of the Walker Circulation: Implications for Projections: *Journal of Climate*, v.28, p.20-35. doi.org/10.1175/JCLI-D-13-00752.1
- Kohyama, T., Hartmann, D.L., and Battisti, D.S., 2017, La Niña-like Mean-State Response to Global Warming and Potential Oceanic Roles: *Journal of Climate*, v.30, p.4207-4225. doi.org/10.1175/JCLI-D-16-0441.1
- Kovats, R.S., 2000, El Niño and human health: *Bulletin of the World Health Organization*, v.78(9), p.1127-1135.
- Kug, J.-S., Jin, F.-F., and An, S.-I., 2009, Two Types of El Niño Events: Cold Tongue El Niño and Warm Pool El Niño: *Journal of Climate*, v.22, p.1499-1515. doi.10.1175/2008JCLI2624.1
- Lawman, A.E., Quinn, T.M., Partin, J.W., Thirumalai, K., Taylor, F.W., Wu, C., Yu, T., Gorman, M.K., and Shen, C., 2020, A Century of Reduced ENSO Variability During the Medieval Climate Anomaly: *Paleoceanography and Paleoclimatology*, v.35, p.1-17. doi.10.1029/2019PA003742
- Larkin, N.K., and Harrison, D.E., 2005, Global seasonal temperature and precipitation anomalies during El Niño autumn and winter: *Geophysical Research Letters*, v.32, p.1-4. doi.10.1029/2005GL022860
- Lea, D.W., Shen, G.T., and Boyle, E.A., 1989, Coralline barium records temporal variability in equatorial Pacific upwelling: *Nature*, v.340, p.373-376. doi.org/10.1038/340373a0
- Li, M., Hinnov, M., and Kump, L., 2019, Acycle: Time-series analysis software for paleoclimate research and education: *Computers & Geosciences*, v.127, p.12-22. doi.org/10.1016/j.cageo.2019.02.011.
- Loope, G., Thompson, D.M., Cole, J.E., and Overpeck, J.T., 2020, Is there a low-frequency bias in multiproxy reconstructions of tropical pacific SST variability?: *Quaternary Science Reviews*, v.246, p.106530. doi.10.1016/j.quascirev.2020.106530
- Lough, J.M., 2004, A strategy to improve the contribution of coral data to high-resolution paleoclimatology: *Palaeogeography, Palaeoclimatology, Palaeoecology*, v.204, p.115-143. doi.org/10.1016/S0031-0182(03)00727-2
- Luo, Y., Lu, J., Liu, F., and Garuba, O., 2017, The Role of Ocean Dynamical Thermostat in Delaying the El Niño-Like Response over the Equatorial Pacific to Climate Warming: *American Meteorological Society*, v.30, p.2811-2827. doi.10.1175/JCLI-D-16-0454.1

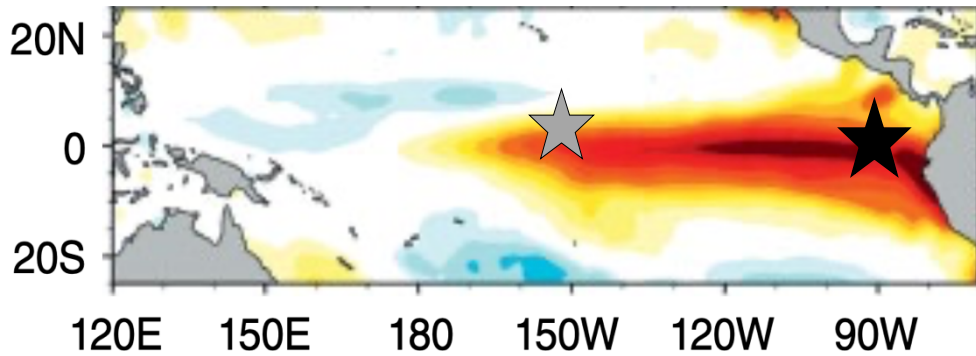
- Mann, M.E., Zhang, Z., Rutherford, S., Bradley, R.S., Hughes, M.K., Shindell, D., Caspar, A., Faluvegi, G., and Ni, F., 2009, Global Signatures and Dynamical Origins of the Little Ice Age and Medieval Climate Anomaly: *Science*, v.326, p.1256-1260. doi.10.1126/science.1177303
- McConnaughey, T., 1989, ^{13}C and ^{18}O isotopic disequilibrium in biological carbonates: II. In vitro simulation of kinetic isotope effects: *Geochimica et Cosmochimica Acta*, v.53, p.163-171. doi.org/10.1016/0016-7037(89)90283-4
- McGregor, S., Timmermann, A., England, M.H., Timm, O.E., and Wittenberg, A.T., 2013, Inferred changes in El Niño Southern Oscillation variance over the past six centuries: *Climate of the Past*, v.9, p.2269–2284. doi.10.5194/cp-9-2269-2013
- McPhaden, M. J., Zebiak, S. E., and Glantz, M. H., 2006, ENSO as an integrating concept in Earth science: *Science*, v.314, p.1740–1745. doi.10.1126/science.1132588
- McPhaden, M.J., Santoso, A., and Cai, W., 2021, Introduction to El Niño Southern Oscillation in a Changing Climate, *in* McPhaden, M.J., Santoso, A., and Cai, W., ed. 1, *El Niño Southern Oscillation in a Changing Climate*, Geophysical Monograph 253: John Wiley & Sons, Inc., p.3-19.
- Moreau, M., Corrège, T., Dassié, E.P., and Le Cornec, F., 2015, Evidence for the non-influence of salinity variability on the Porites coral Sr/Ca palaeothermometer: *Climate of the Past*, v.11, p.523-532. doi.org/10.5194/cp-11-523-2015
- Newman, M., S.-I., Shin, and Alexander, M.A., 2011, Natural variation in ENSO flavors: *Geophysical Research Letters*, v.38, p.1-7. doi.10.1029/2011GL047658
- Nurhati, I.S., Cobb, K.M., Charles, C.D., and Dunbar, R.B., 2009, Late 20th century warming and freshening in the central tropical Pacific: *Geophysical Research Letters*, v.36, p.1-4. doi.10.1029/2009GL040270
- Parzen, E., 1962, On estimation of a probability density function and mode: *Annals of Mathematical Statistics*, v.33(3), p.1065-1076. doi.10.1214/amos/1177704472
- Plesca, E., Buehler, S.A., and Grützun, V., 2018, The Fast Response of the Tropical Circulation to CO₂ Forcing: *Journal of Climate*, v.31, p.9903-9920. doi.org/10.1175/JCLI-D-18-0086.1
- Power, S., Delage, F., Wang, G., Smith, I., and Kociuba, G., 2017, Apparent limitations in the ability of CMIP5 climate models to simulate recent multi-decadal change in surface temperature: implications for global temperature projections: *Climate Dynamics*, v.49, p.53–69. doi.org/10.1007/s00382-016-3326-x
- Rasmusson, E.M. and Carpenter, T.H., 1982, Variations in Tropical Sea Surface Temperature and Wind Associated with the Southern Oscillation/El Niño: *Monthly Weather Review*, v.110, p.354-384. doi.org/10.1175/1520-0493(1982)110<0354:VITSST>2.0.CO;2
- Rayner, N.A., Parker, D.E., Horton, E.B., Folland, C.K., Alexander, L.V., Rowell, D.P., Kent, E.C., and Kaplan, A., 2003, Global analyses of sea surface temperature, sea ice, and night marine air temperature since the late nineteenth century: *Journal of Geophysical Research: Atmospheres*, v.108, p.1-37. doi.10.1029/2002JD002670
- Reed, E.V., Thompson, D.M., Cole, J.E., Lough, J.M., Cantin, N.E., Cheung, A.H., Tudhope, A., Vetter, L., Jimenez, G., and Edwards, R.L., 2021, Impacts of Coral Growth on Geochemistry: Lessons from the Galápagos Islands: *Paleoceanography and Paleoclimatology*, Accepted Articles, p.1-40. doi.10.1029/2020PA004051
- Reynolds, R. W., Rayner, N.A., Smith, T. M., Stokes, D.C., and Wang, W., 2002, An improved in situ and satellite SST analysis for climate: *Journal of Climate*, v.15, p.1609–1625. doi.10.1175/1520-0442(2002)015<1609:AIISAS>2.0.CO;2

- Ribsey, J.S., Pook, M., McIntosh, P.C., and Wheeler, M.C., 2009, On the Remote Drivers of Rainfall Variability in Australia: *American Meteorological Society*, v.137, p.3233-3253. doi.10.1175/2009MWR2861.1
- Rustic, G.T., Koutavas, A., Marchitto, T.M., and Linsley, B.K., 2015, Dynamical excitation of the tropical Pacific Ocean and ENSO variability by Little Ice Age cooling: *Paleoceanography*, v.35, p.1537-1541. doi.10.1126/science.aac9937
- Sanchez, S.C., Westphal, N., Haug, G.H., Cheng, H., Edwards, R.L., Schneider, T., Cobb, K.M., and Charles, C.D., 2020, A Continuous Record of Central Tropical Pacific Climate Since the Midnineteenth Century Reconstructed From Fanning and Palmyra Island Corals: A Case Study in Coral Data Reanalysis: *Paleoceanography and Paleoclimatology*, v.35, p.1-15. doi.10.1029/2020PA003848
- Sachs, J.P., Sachse, D., Smittenberg, R., and Zhang, Z., 2009, Southward movement of the Pacific intertropical convergence zone AD 1400–1850: *Nature Geoscience*, v.2, p.519-525. doi.10.1038/ngeo554
- Santoso, A., McPhaden, M. J., & Cai, W., 2017, The defining characteristics of ENSO extremes and the strong 2015/16 El Niño: *Reviews of Geophysics*, v.55, p.1079–1129. doi.org/10.1002/2017RG000560
- Schrag, D.P., Rapid analysis of high-precision Sr/Ca ratios in corals and other marine carbonates: *Paleoceanography*, v.14, p.97-103. doi.org/10.1029/1998PA900025
- Shen, G.T., Boyle, E.A., and Lea, D.W., 1987, Cadmium in corals as a tracer of historical upwelling and industrial fallout: *Nature*, v.328, p.794-796. doi.org/10.1038/328794a0
- Sweet, W. V., Morrison, J. M., Kamykowski, D., Schaeffer, B. A., Banks, S., and McCulloch, A., 2007, Water mass seasonal variability in the Galapagos archipelago: *Deep-Sea Research Part I*, v.54, p. 2023–2035. doi.org/10.1016/j.dsr.2007.09.009
- Takahashi, K., Montecinos, A., Goubanova, A., and Dewitte, B., 2011, ENSO regimes: Reinterpreting the canonical and Modoki El Niño: *Geophysical Research Letters*, v.38, p.1-5. doi.10.1029/2011GL047364
- Thirumalai, K., Partin, J.W., Jackson, C.S., and Quinn, T.M., 2013, Statistical constraints on El Niño Southern Oscillation reconstructions using individual foraminifera: A sensitivity analysis: *Paleoceanography*, v.28, p.401-412. doi.10.1002/palo.20037
- Tierney, J.E., Abram, N.J., Anchukaitis, K.J., Evans, M.N., Giry, C., Kilbourne, K.H., Saenger, C.P., Wu, H.C., and Zinke, J., 2015, Tropical sea surface temperatures for the past four centuries reconstructed from coral archives: *Paleoceanography*, v.30, p.226-252. doi.org/10.1002/2014PA002717
- Trenberth, K. E., Branstator, G. W., Karoly, D., Kumar, A., Lau, N. C., and Ropelewski, C., 1998, Progress during TOGA in understanding and modeling global teleconnections associated with tropical sea surface temperatures: *Journal of Geophysical Research*, v.10, p.14,291–14,324. doi.org/10.1029/97JC01444
- Trenberth, K. E., 1997, The definition of El Niño: *Bulletin of the American Meteorological Society*, v.78(12), p.2771–2777. doi.10.1175/1520-0477(1997)078<2772:TDOENO>2.0.CO;2
- Trueman, M., and d’Ozouville, N., 2010, Characterizing the Galapagos terrestrial climate in the face of global climate change: *Galapagos Research*, v.67, p.26-37.
- Tudhope, A.W., Chilcott, C.P., McCulloch, M.T., Cook, E.R., Chappell, J., Ellam, R.M., Lea, D.W., Lough, J.M., and Shimmield, G.B., 2001, Variability in the El Niño Southern Oscillation Through a Glacial-Interglacial Cycle: *Science*, v.291, p.1511-1517. doi.10.1126/science.1057969
- Vecchi, G.A., and Soden, B.J., 2007, Increased tropical Atlantic wind shear in model projections of global warming: *Geophysical Research Letters*, v.34, p.1-5. doi.10.1029/2006GL028905

- Vecchi, G.A., and Wittenberg, A.T., 2010, El Niño and our future climate: Where do we stand?: Wiley Interdisciplinary Reviews Climate Change: v.1, p.260-270. doi.10.1002/wcc.33
- Wang, C., Deser, C., Yu, J.-Y., DiNezio, P., and Clement, A., 2017, El Niño and Southern Oscillation (ENSO): A Review, *in* P.W. Glynn et al., ed.8, Coral Reefs of the Eastern Tropical Pacific, Coral Reefs of the World: Springer Science + Business Media Dordrecht 2017, p.85-106. doi.10.1007/978-94-017-7499-4_4
- Wang, B., Luo, X., Yang, Y.-M., Sun, W., Cane, M.A., Cai, W., Yeh, S.-W., and Liu, J., 2019, Historical change of El Niño properties sheds light on future changes of extreme El Niño: Proceedings of the National Academy of Sciences, v.116, p. 22512–22517. doi.10.1073/pnas.1911130116
- Weber, J.N., and Woodhead, P.M.J., 1972, Temperature dependence of oxygen-18 concentration in reef coral carbonates: Journal of Geophysical Research, v.77, p.463-473. doi. org/10.1029/JC077i003p00463
- Wellington, G.M., Dunbar, R.B., and Merlen, G., 1996, Calibration of stable oxygen isotope signatures in Galápagos corals: Paleoceanography, v.11, p.467-480. doi.org/10.1029/96PA01023
- Wittenberg, A. T., 2009, Are historical records sufficient to constrain ENSO simulations?: Geophysical Research Letters, v.36, p.2702. doi.10.1029/2009GL038710
- Wolff, M., 2010, Galapagos does not show recent warming but increased seasonality: Galapagos Research, v.67, p.38–44.
- Wu, H.C., Linsley, B.K., Dassié, E.P., Schiraldi, B., and deMenocal, P.B., 2013, Oceanographic variability in the South Pacific Convergence Zone region over the last 210 years from multi-site coral Sr/Ca records: Geochemistry, Geophysics, Geosystems, v.14, p.1435-1453. doi.org/10.1029/2012GC004293
- Xie, S.-P., Okumura, Y., Miyama, T., and Timmerman, A., 2008, Influences of Atlantic Climate Change on the Tropical Pacific via the Central American Isthmus, v.21, p.3914-3928. doi.org/10.1175/2008JCLI2231.1
- Yan, H., Wei, W., Soon, W., An, Z., Zhou, W., Liu, Z., Wang, Y., and Carter, R.M., 2015, Dynamics of the intertropical convergence zone over the western Pacific during the Little Ice Age: Nature, v.8, p.315-320. doi.org/10.1038/ngeo2375
- Yeh, S.-W., Cai, W., Min, S.-K., McPhaden, M. J., Dommenges, D., Dewitte, B., Collins, M., Ashok, K., Soon-Il, A., Yim, B.-Y., and Kug, J.-S., 2018, ENSO atmospheric teleconnections and their response to greenhouse gas forcing: Reviews of Geophysics, v.56, p.185-206. doi.10.1002/2017RG000568
- Yeh, S.-W., Kirtman, B.P., Kug, J.-S., Park, W., and Latif, M., 2011, Natural variability of the central Pacific El Niño event on multi-centennial timescales: Geophysical Research Letters, v.38, p.1-5. doi.10.1029/2010GL045886
- Yeh, S.-W., Kug, J.-S., Dewitte, B., Kwon, M.-H., Kirtman, B. P., and Jin, F.-F., 2009, El Niño in a changing climate: Nature, v.461, p.511-514. doi.10.1038/nature08316
- Zhang, R., A. Sumi, and M. Kimoto, 1996, Impact of El Niño on the East Asian monsoon: A diagnostic study of the '86/87 and '91/92 events: Japan Meteorological Society, Japan, v.74, p.49–62. doi.org/10.2151/jmsj1965.74.1_49

FIGURES

A) DJF 1997/1998 EP El Niño Event



B) DJF 2009/2010 CP El Niño Event

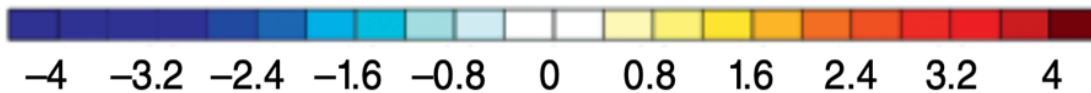
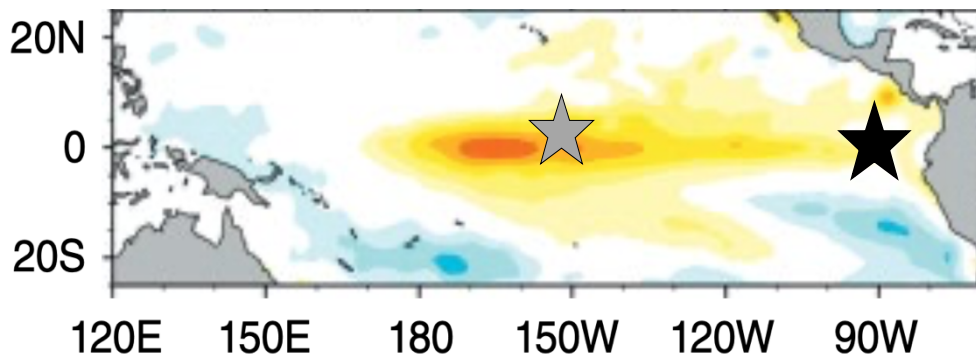


Figure 1. Interannual SST anomalies spanning December-January-February (DJF) during **A)** an EP El Niño event and **B)** a CP El Niño event in the tropical Pacific Ocean. Gray star represents the Northern Line Islands, and black star represents the Galápagos. Monthly SST data were obtained from the NOAA Optimum Interpolation (OISST) data set (Reynolds et al., 2002). Anomalies are computed relative to the 1982–2017 climatology. Gathered and modified from Capotondi et al., 2021.

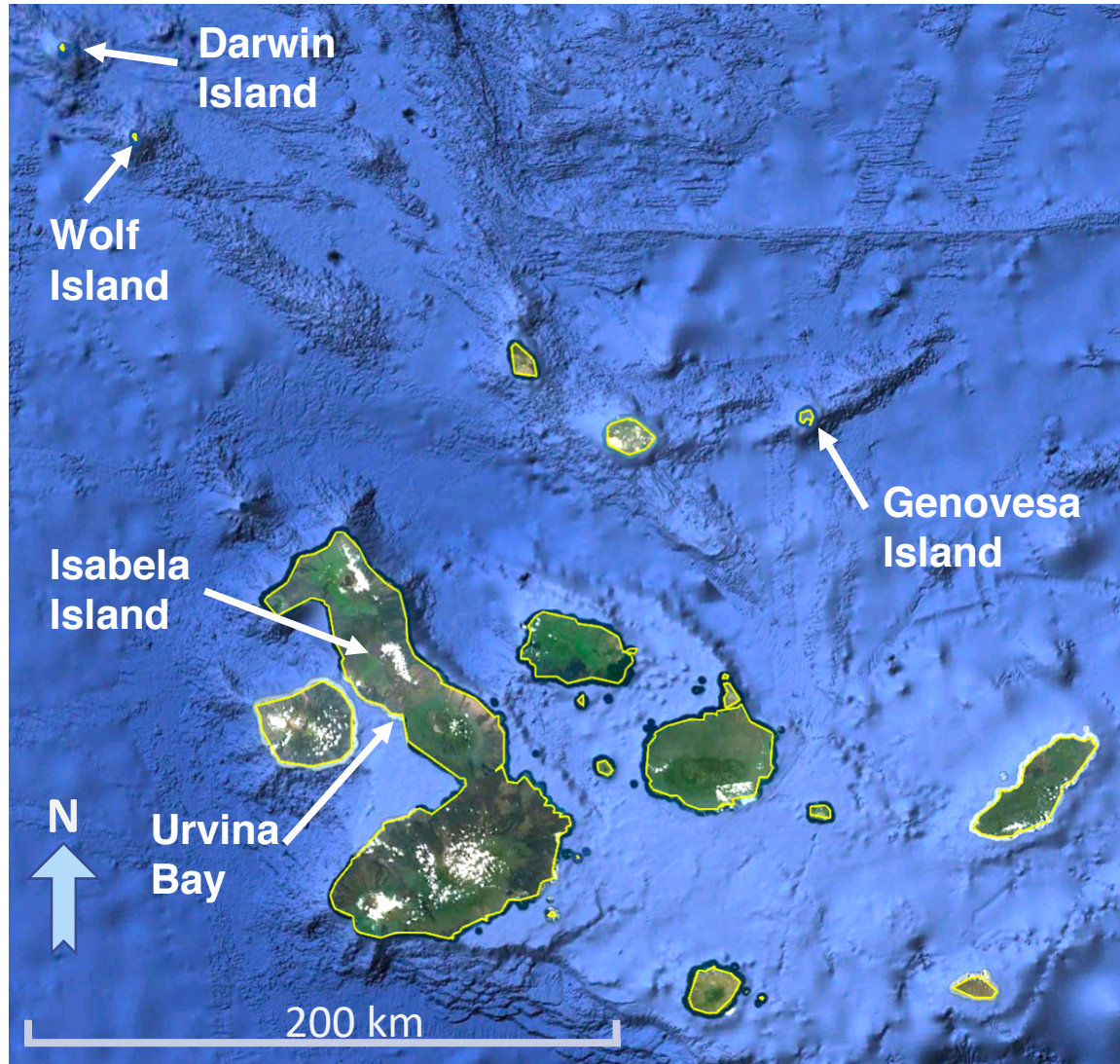


Figure 2. Map of the Galápagos archipelago. Gathered from Google Earth, 2021

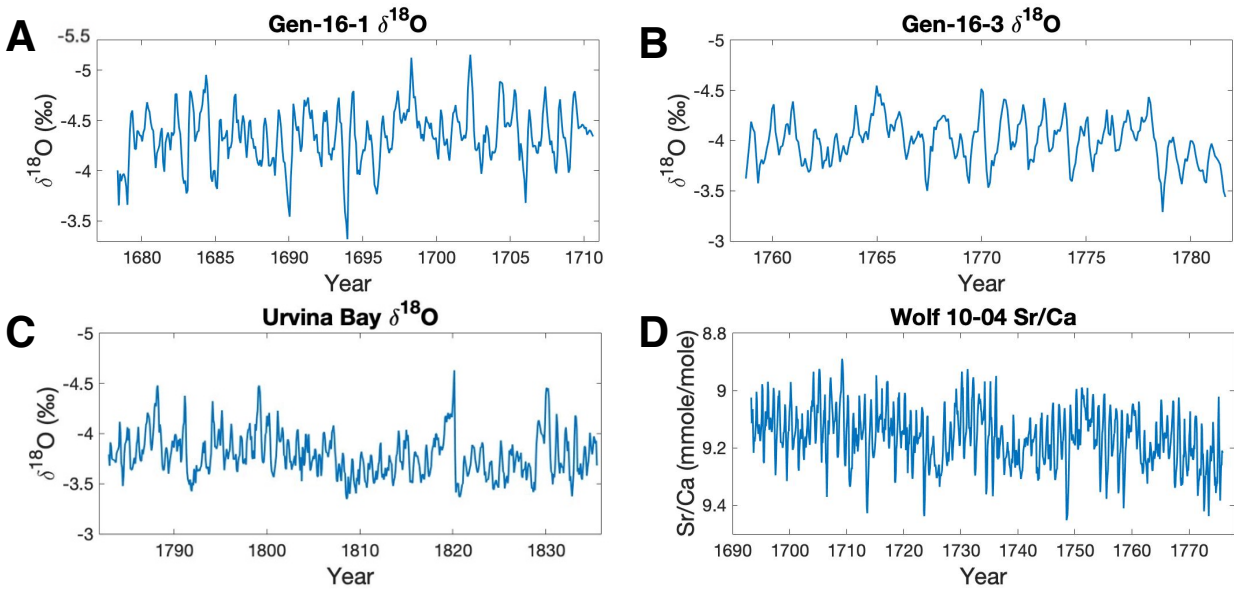


Figure. 3A-D. New (or re-published) eastern Pacific raw $\delta^{18}\text{O}$ or Sr/Ca records of fossil Galápagos coral records. **A)** Genovesa Island core 1 (32 years; this study); **B)** Genovesa Island core 3 (23 years; this study); **C)** Urvina Bay core UR-86 (52 years; Druffel et al., 2015); **D)** Wolf Island core 10-04 (83 years; Reed et al., 2021).

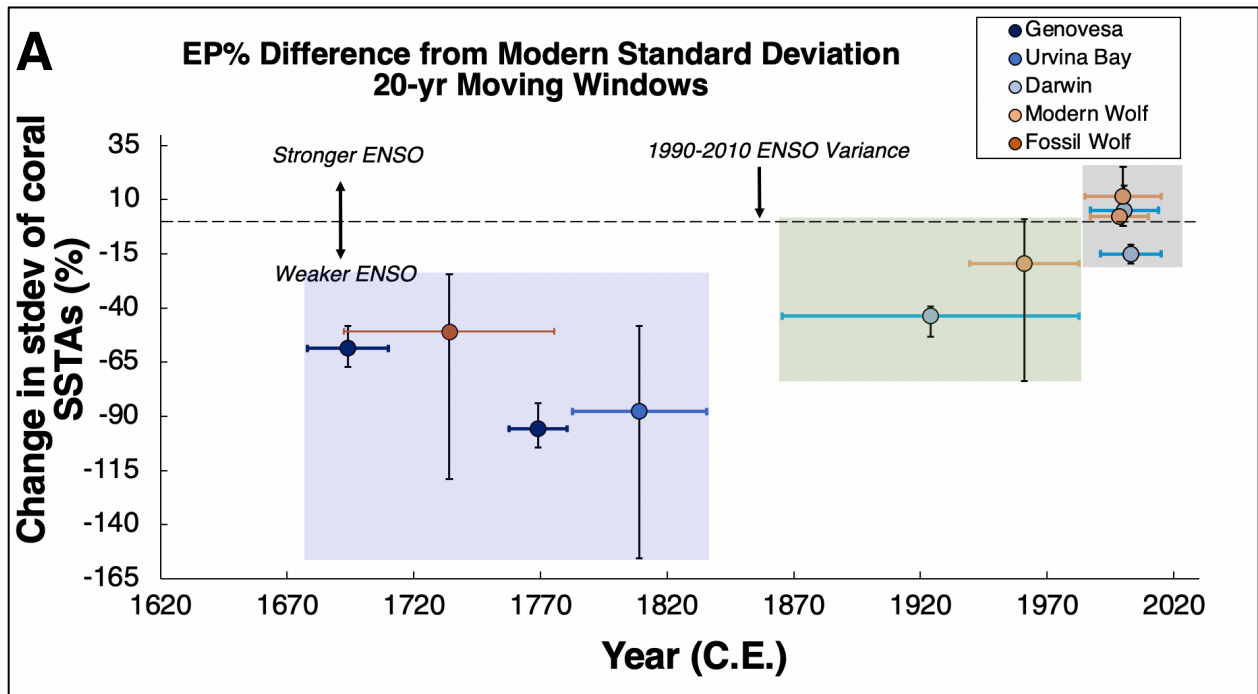


Figure 4A. Relative interannual ENSO variability changes of the eastern tropical Pacific Ocean spanning the 17th-21st centuries. All records were filtered using a 2-7 year bandpass and a 20-month running average was applied. Points represent the average standard deviation of each record and are centered on the middle year of each record. Horizontal lines correspond with record length, vertical lines show the maximum and minimum standard deviation values of each record. Y-axis represents the percent difference in standard deviation from modern. Dashed line is the average of modern coral variability from 1990-2010 CE, taken from Wolf 10-10, Wolf 10-03 (Jimenez et al., 2018), GD15 3-1 (Cheung et al., unpublished), and GD15 3-2 (Jimenez, 2019; 1991-2010 was used for this record). Blue shading represents the “fossil” interval, green the “20th century,” and gray the “recent modern.” See Table S1A for a summary of all records and original citations.

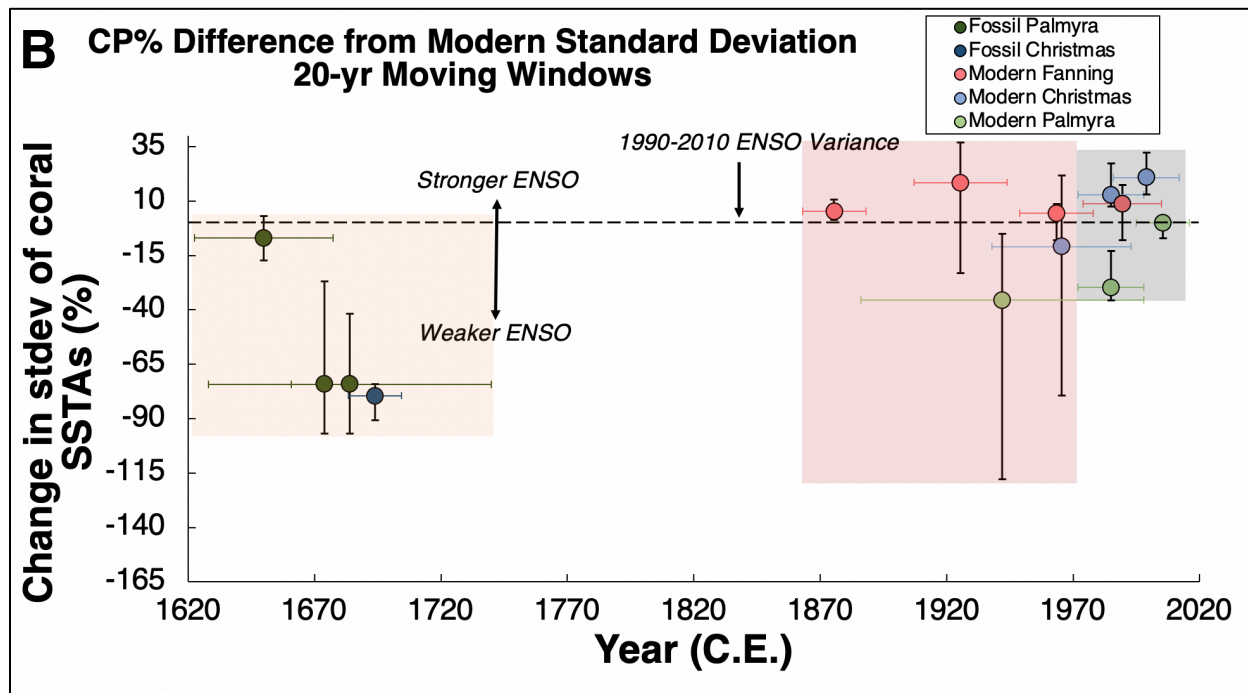


Figure 4B. Same as above but using tropical central Pacific Ocean records. Dashed line is the average of modern coral variability from 1990-2010 CE, taken from the spliced Palmyra (Sanchez et al., 2020) and spliced Christmas (Grothe et al., 2019) modern records (not plotted), and the Christmas X12-6 record (Grothe et al., 2019). Orange shading represents the “fossil” interval, red the “20th century,” and gray the “recent modern.” See Table S1B for a summary of all records and original citations.

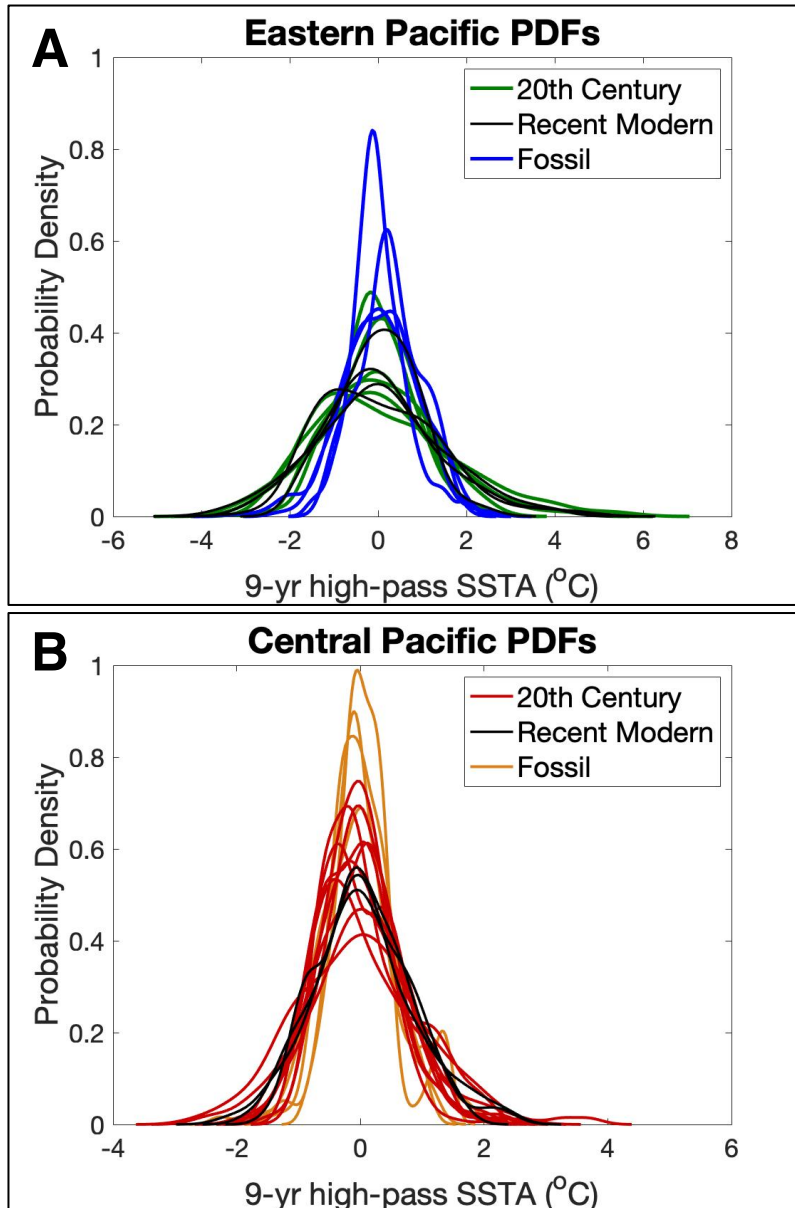


Figure 5A-B. Compiled “fossil,” “20th century,” and “recent modern” PDF distribution curves of the **A**) eastern and **B**) central Pacific Ocean coral records. “Recent modern” curves represent the 1990-2010 PDF window extracted from Wolf 10-10, Wolf 10-03 (Jimenez et al., 2018), Darwin GD15 3-1 (Cheung et al., unpublished), and Darwin GD15 3-2 (Jimenez, 2019) in the EP, and from the spliced Palmyra (Sanchez et al., 2020) and Christmas (Grothe et al., 2019) records, and the Christmas X12-6 record (Grothe et al., 2019) in the CP. Plotted records summarized in Table S1, and spread values listed in Table S3.

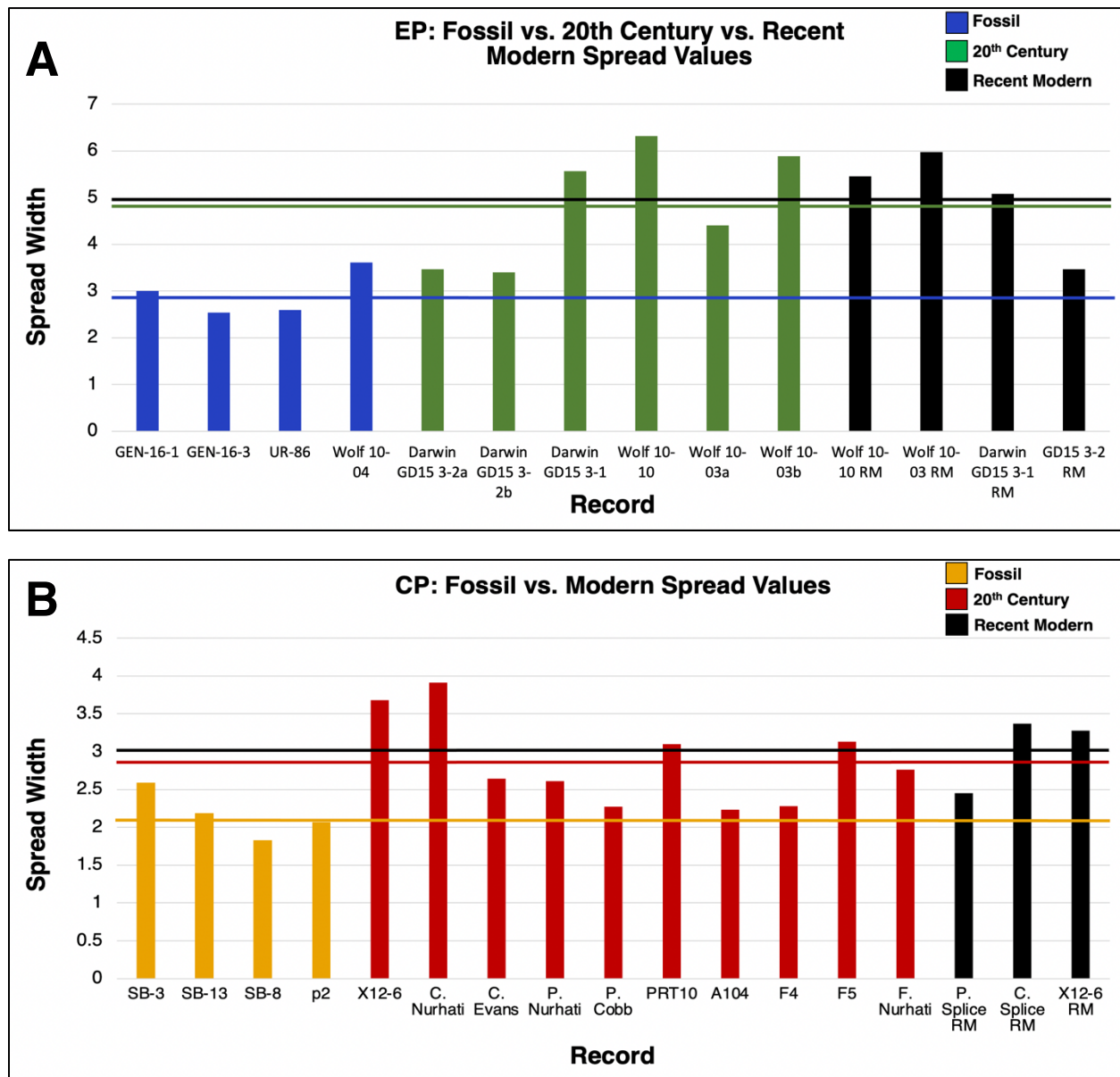


Figure 6A-B. Bars show the PDF spread value of each record from the **A)** eastern Pacific and **B)** central Pacific, comparing the “fossil,” “20th century,” and “recent modern” intervals. Bold horizontal lines show the average spread value of each set of records, which are summarized in Table S1. Spread values represented by each bar are listed in Table S3. “Recent modern” bars represent the 1990-2010 PDF window extracted from Wolf 10-10, Wolf 10-03, Darwin GD15 3-1, and Darwin GD15 3-2 in the EP, and from the Palmyra and Christmas modern spliced records, and the Christmas X12-6 record in the CP.

SUPPLEMENTARY MATERIAL

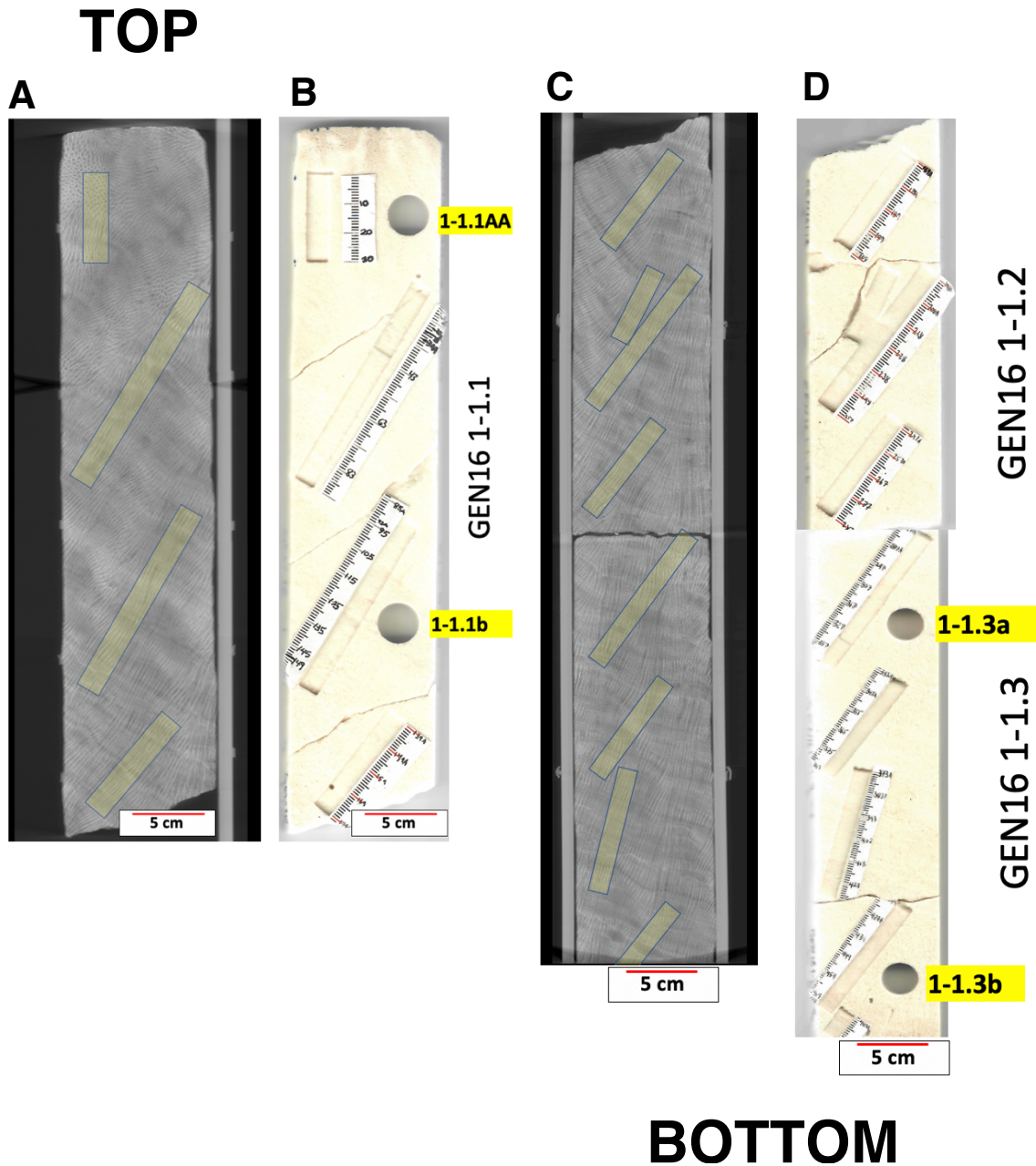


Figure S1A-D. A,C) Slab-averaged CT scan or B,D) photographs of Genovesa Island Core 16-1. Transects are highlighted in yellow and reflect sampling through the best axis of vertical coral growth. Samples were taken at 1mm increments. Top of the core is the youngest. Large holes in the core image (right) represent SEM sample locations. Yellow tags correspond with SEM labels in Figure S2A.

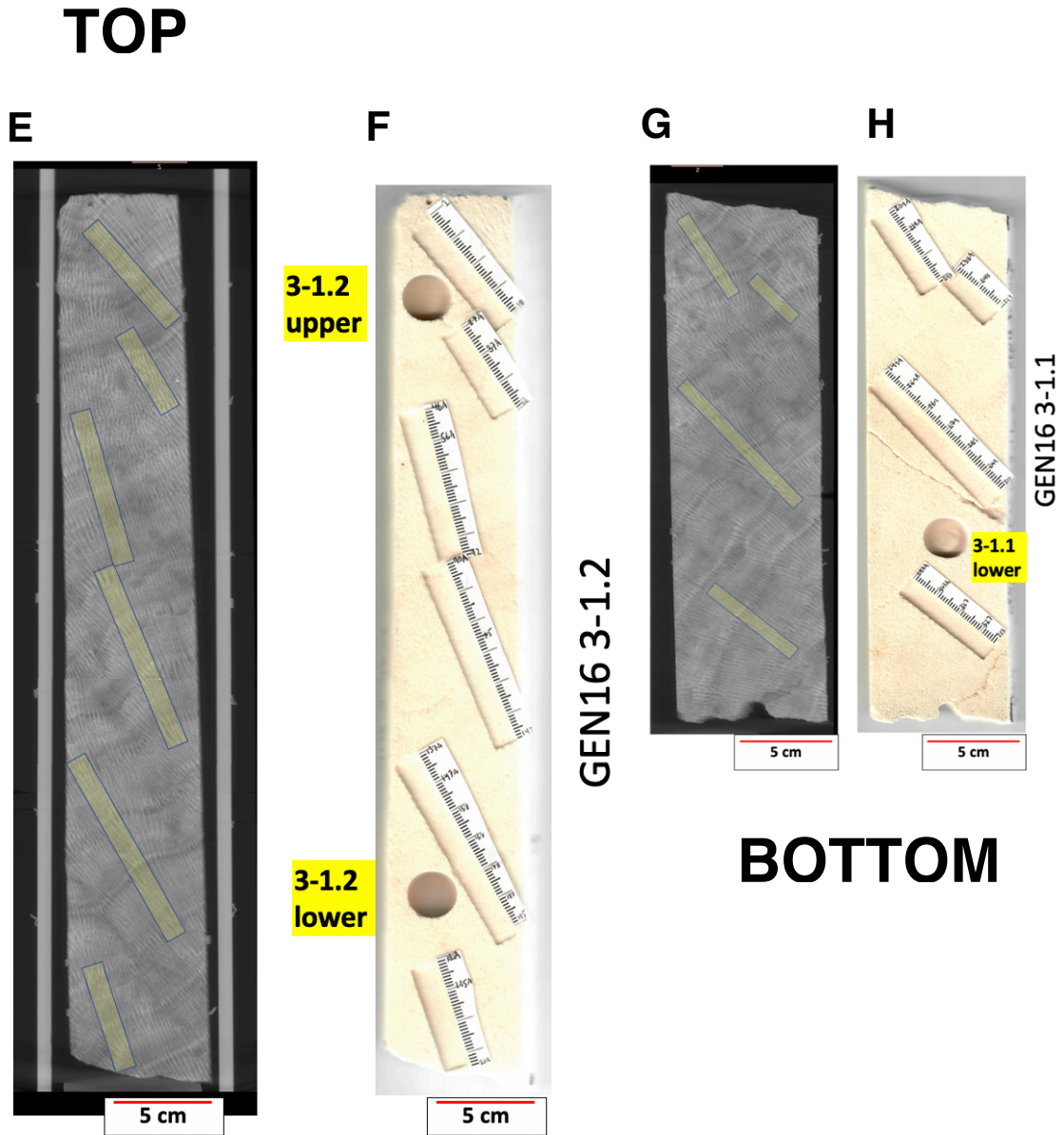


Figure S1E-H. E,G) Slab-averaged CT scan or F,H) photographs of Genovesa Island Core 16-3. Transects are highlighted in yellow and reflect sampling through the best axis of vertical coral growth. Samples were taken at 1mm increments. Top of the core is the youngest. Large holes in the core image (right) represent SEM sample locations. Yellow tags correspond with SEM labels in Figure S2B.

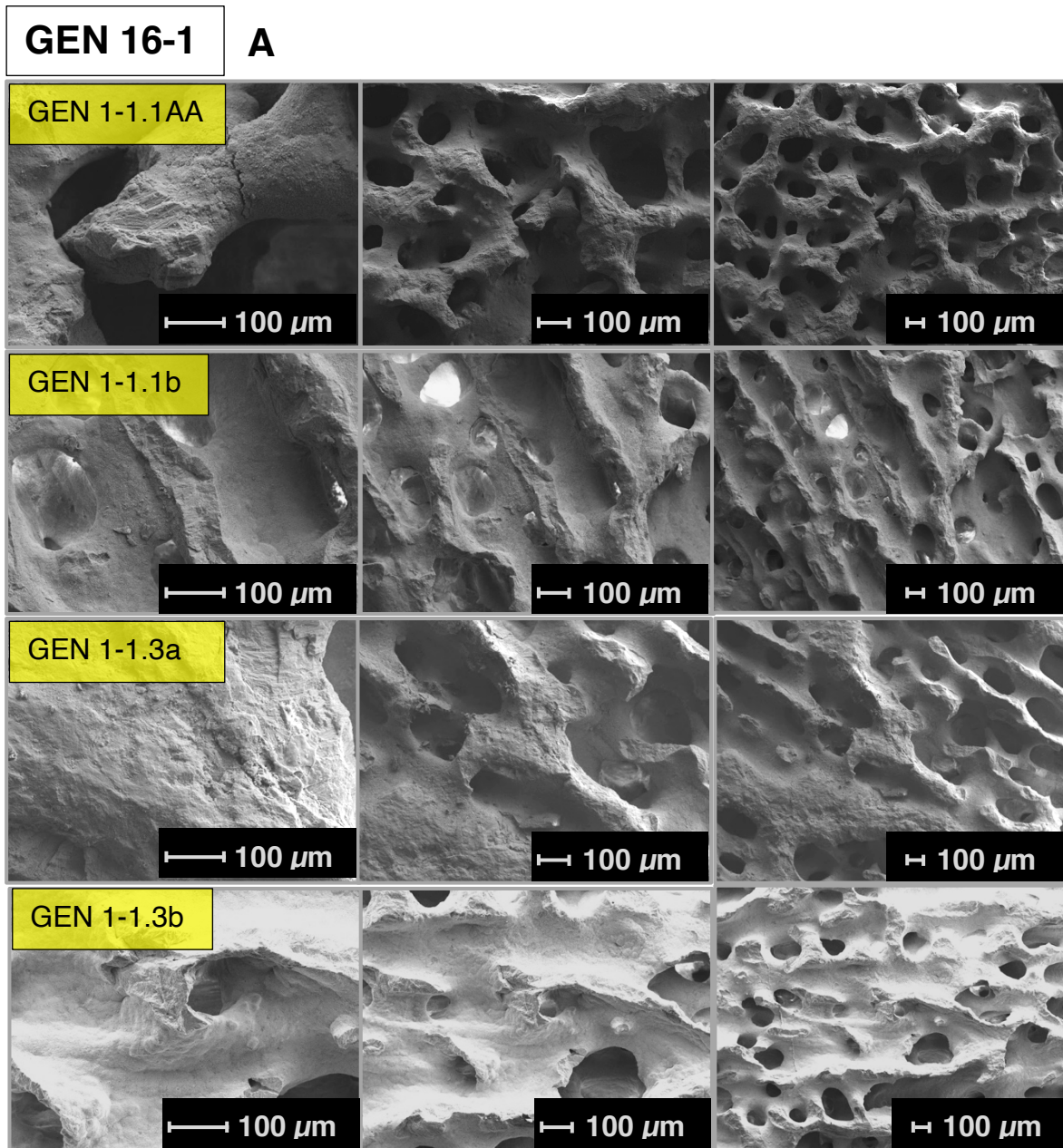


Figure S2A. A series of SEM images collected from Genovesa Island fossil coral core 1 (GEN-16-1).

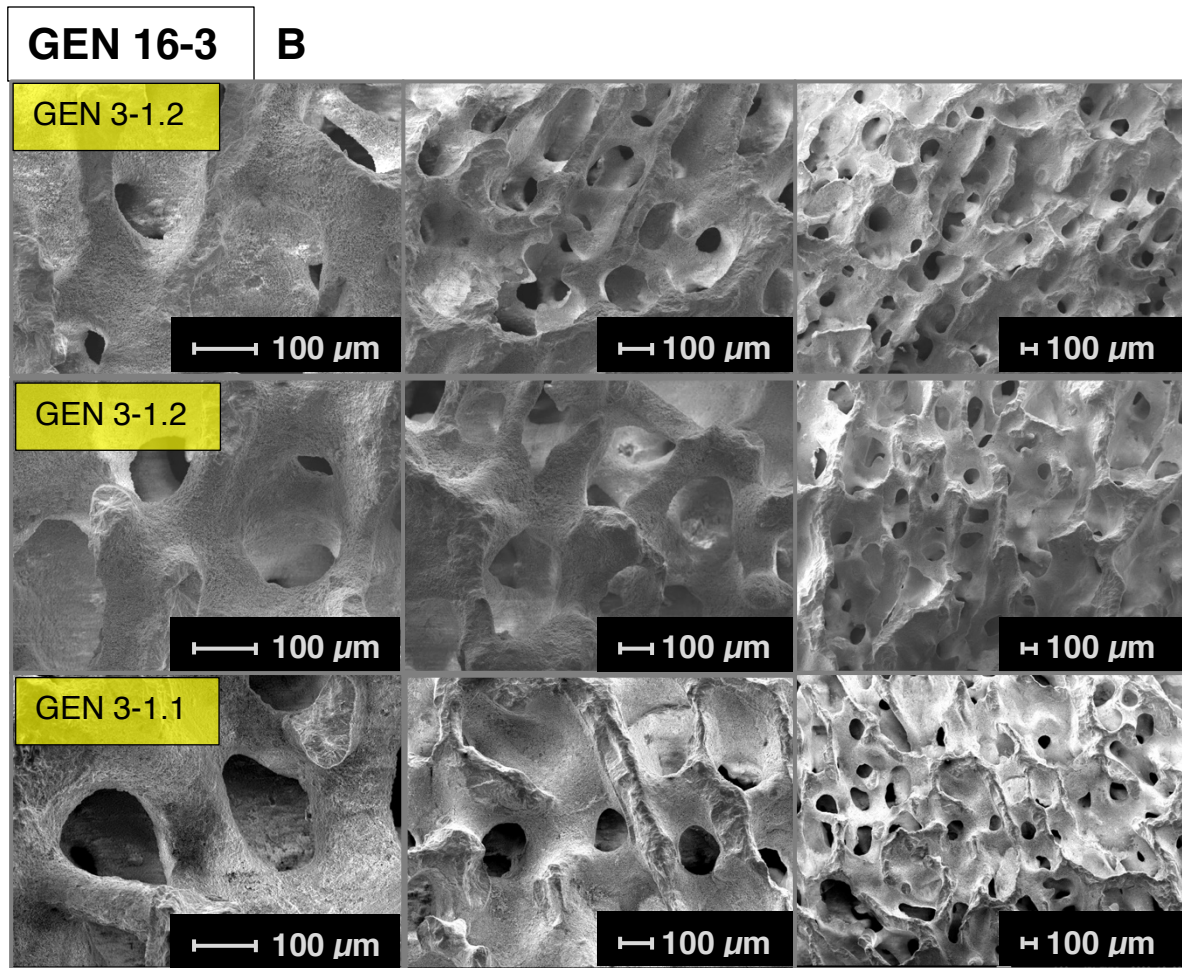


Figure S2B. A series of SEM images collected from Genovesa Island fossil coral core 3 (GEN-16-3).

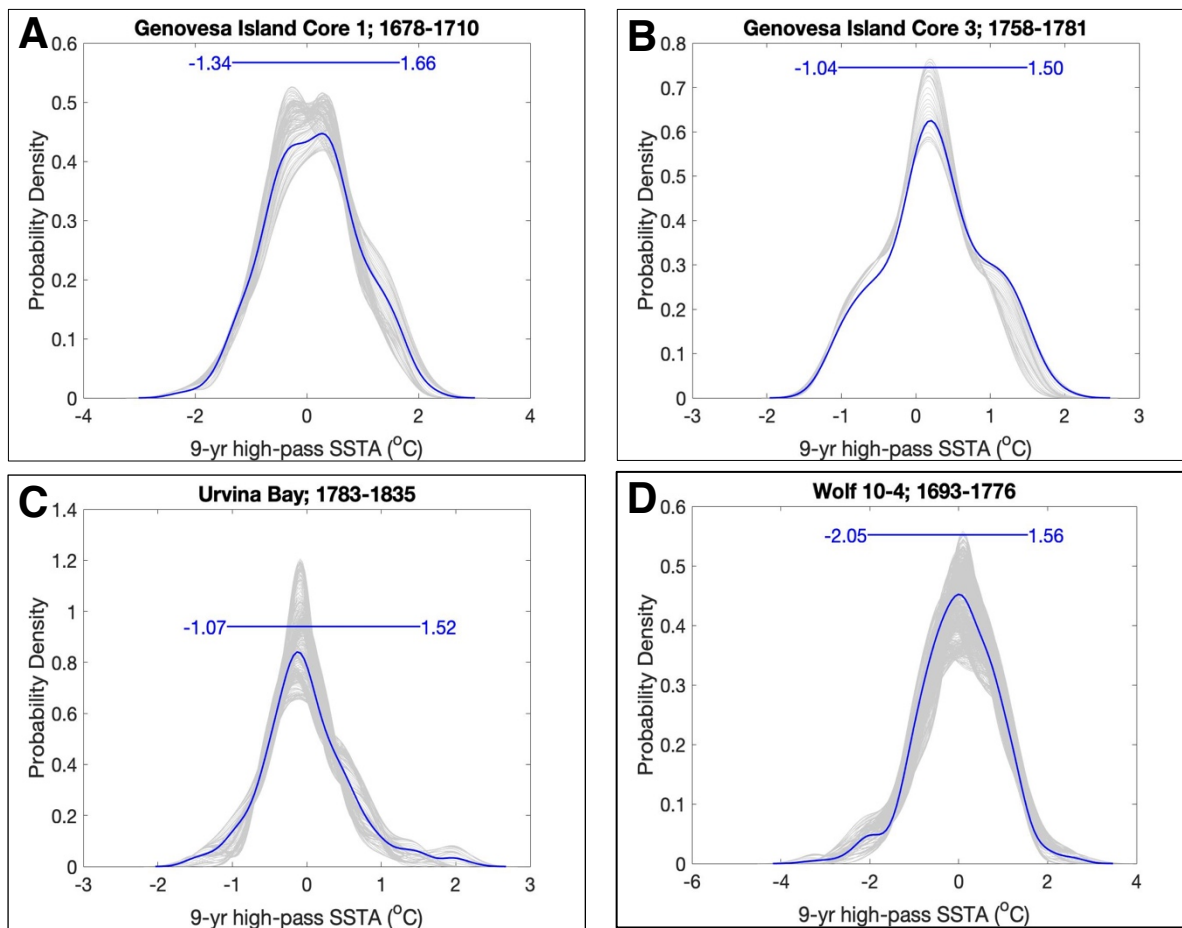


Figure S3A-D. Probability density functions (PDFs) of 17th-18th century “fossil” coral records from the eastern Pacific Ocean (Galápagos region): **A**) core GEN16-1 (32 yrs); **B**) core GEN 16-3 (23 yrs); **C**) Urvina Bay (52 yrs; Druffel et al. 2015); **D**) Wolf 10-04 (83 yrs; Reed et al. 2021). All data have been filtered with a 9-year high pass and smoothed with a 9-month running average. Blue horizontal lines represent the width of the 95th percentile of SSTAs over the full record, and blue numbers denote the 2.5th and 97.5th percentile values. Thick blue curved lines represent PDF distribution over the full length of the record, and thin gray curved lines are PDFs of 20-year moving windows of filtered SSTA data. Windows are shifted at 1-month increments, and each gray curve captures the probability density distribution of a 20-yr window.

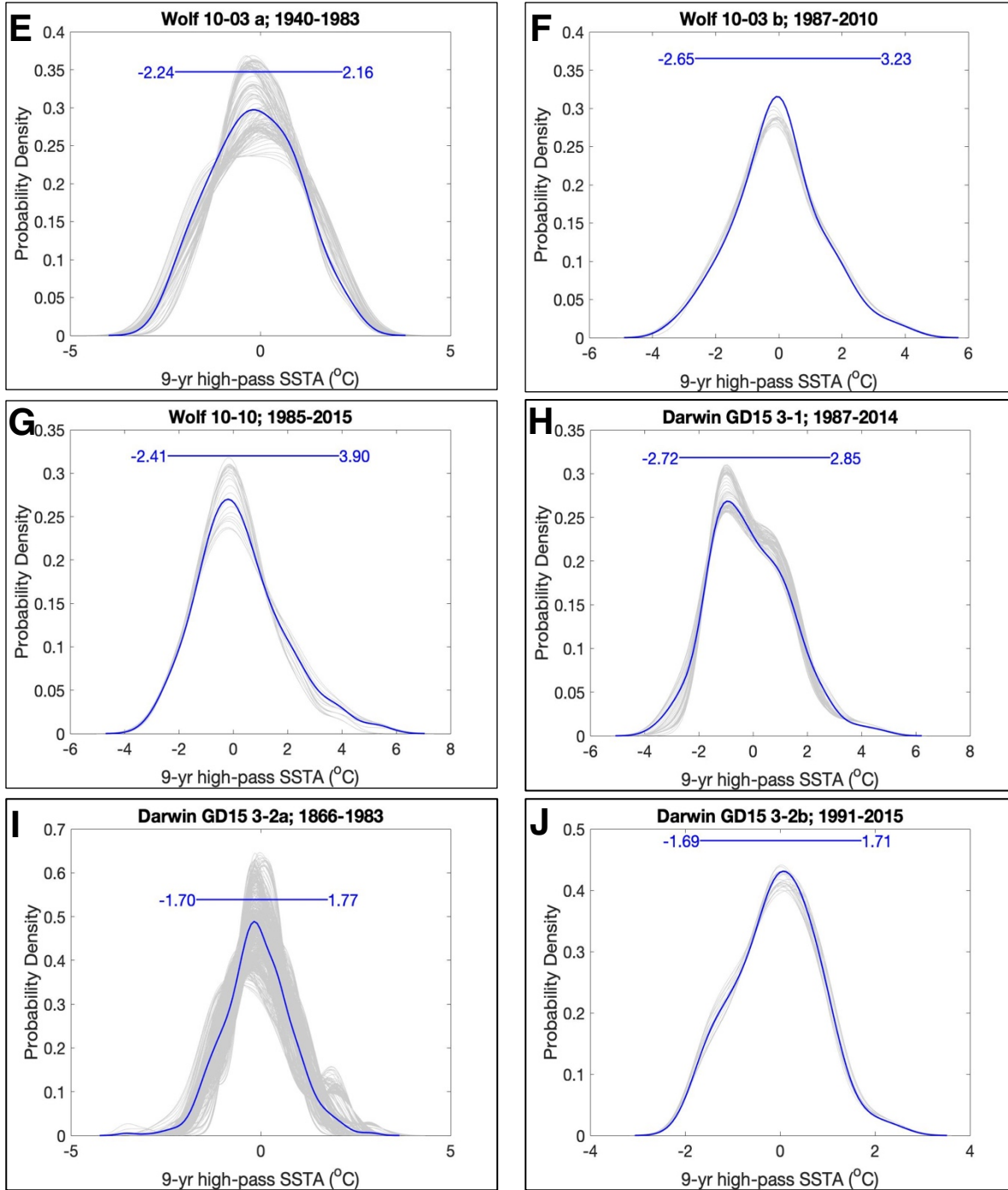


Figure S3E-J. Same as above, but “20th century” coral records from the eastern Pacific Ocean. Data are taken from Wolf Island and Darwin Island in the Galápagos region: **E**) core Wolf 10-03a (43 yrs; Jimenez et al., 2018); **F**) core Wolf 10-03b (23 yrs; Jimenez et al., 2018); **G**) core Wolf 10-10 (30 yrs; Jimenez et al., 2018); **H**) core GD15 3-1 (27 yrs; Cheung et al., unpublished); **I**) core GD15 3-2a (117 yrs; Jimenez, 2019); **J**) core GD15 3-2b (24 yrs; Jimenez, 2019).

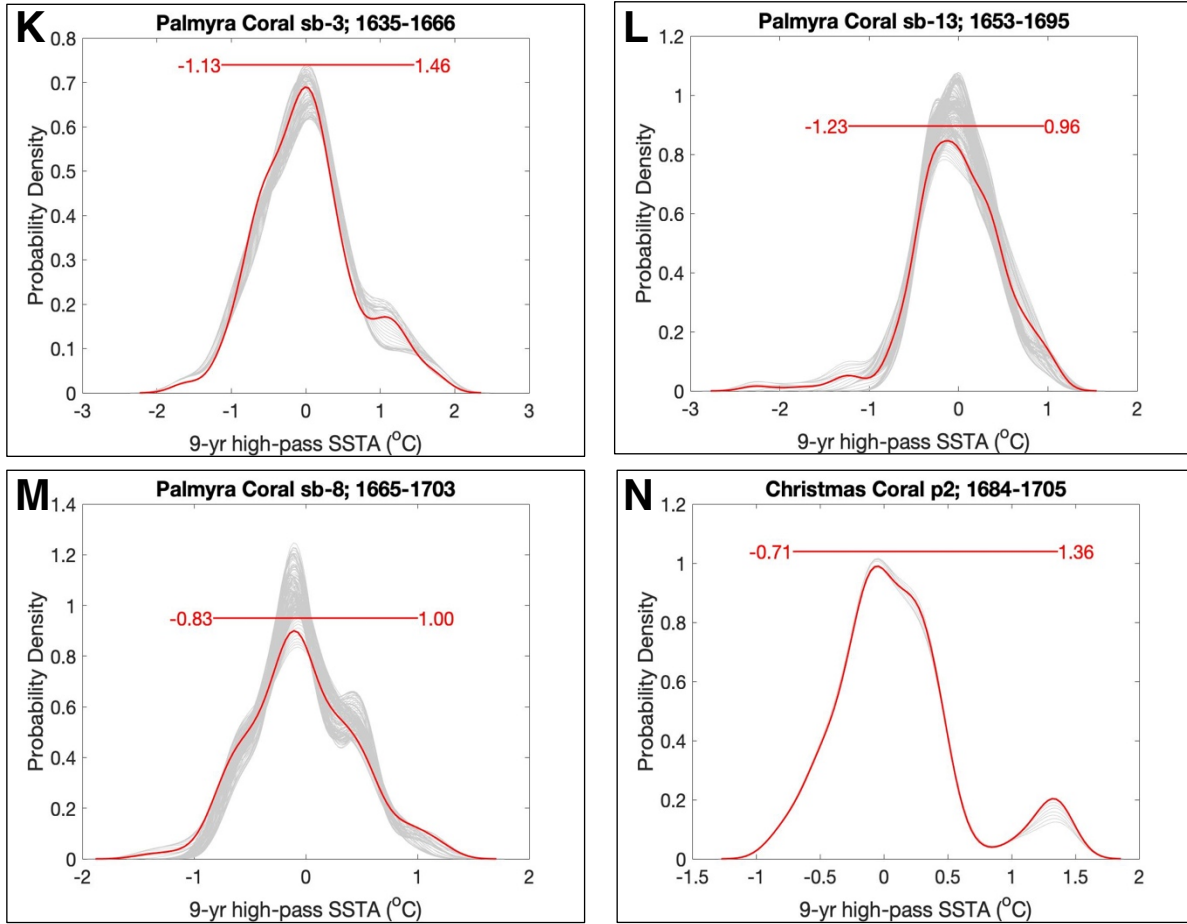
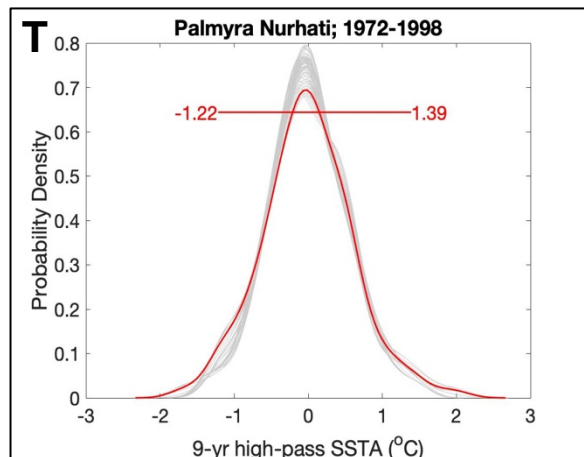
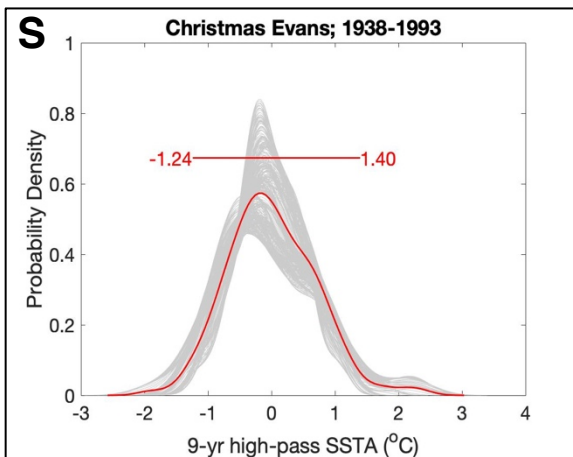
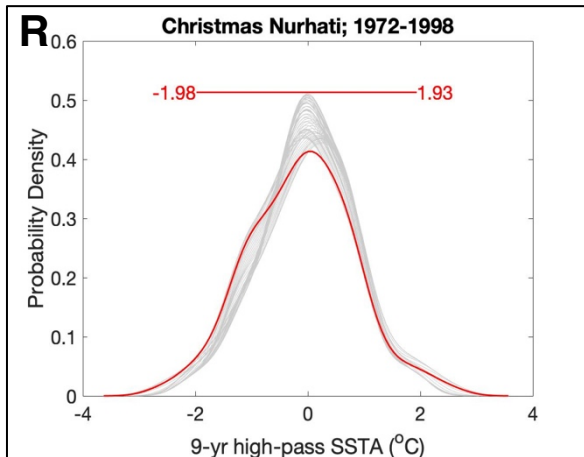
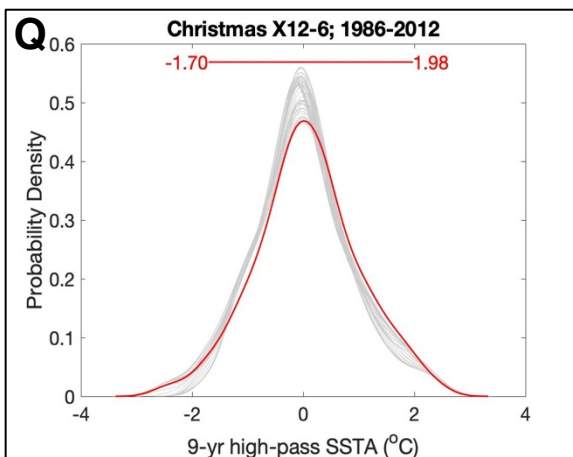
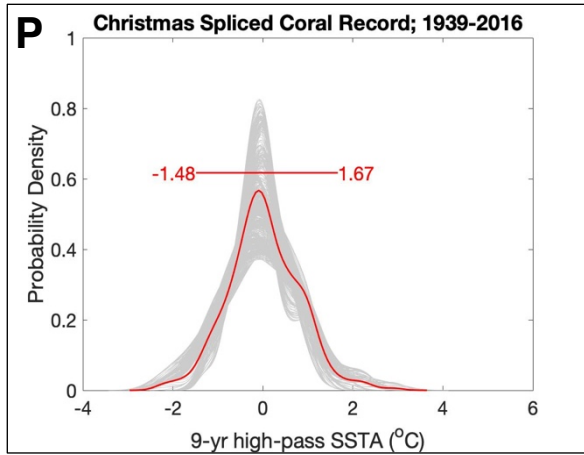
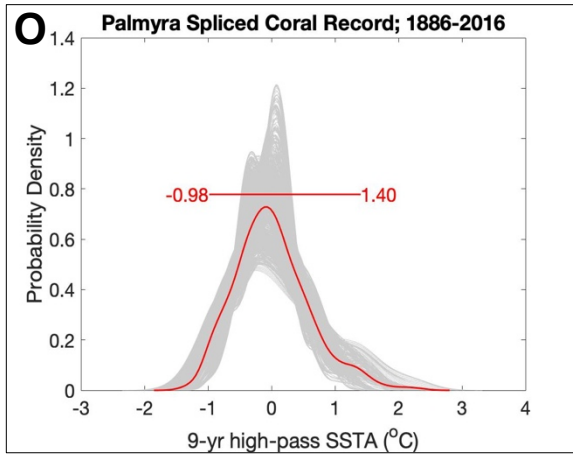


Figure S3K-N. Same as above, but “fossil” coral records from the central Pacific Ocean. Data are taken from Palmyra and Christmas Islands in the Northern Line Islands: **K**) core Palmyra sb-3 (31 yrs; Cobb et al., 2003); **L**) core Palmyra sb-13 (42 yrs; Cobb et al., 2003); **M**) core Palmyra sb-8 (38 yrs; Cobb et al., 2003); **N**) core Christmas p2 (21 yrs; Cobb et al., 2013).



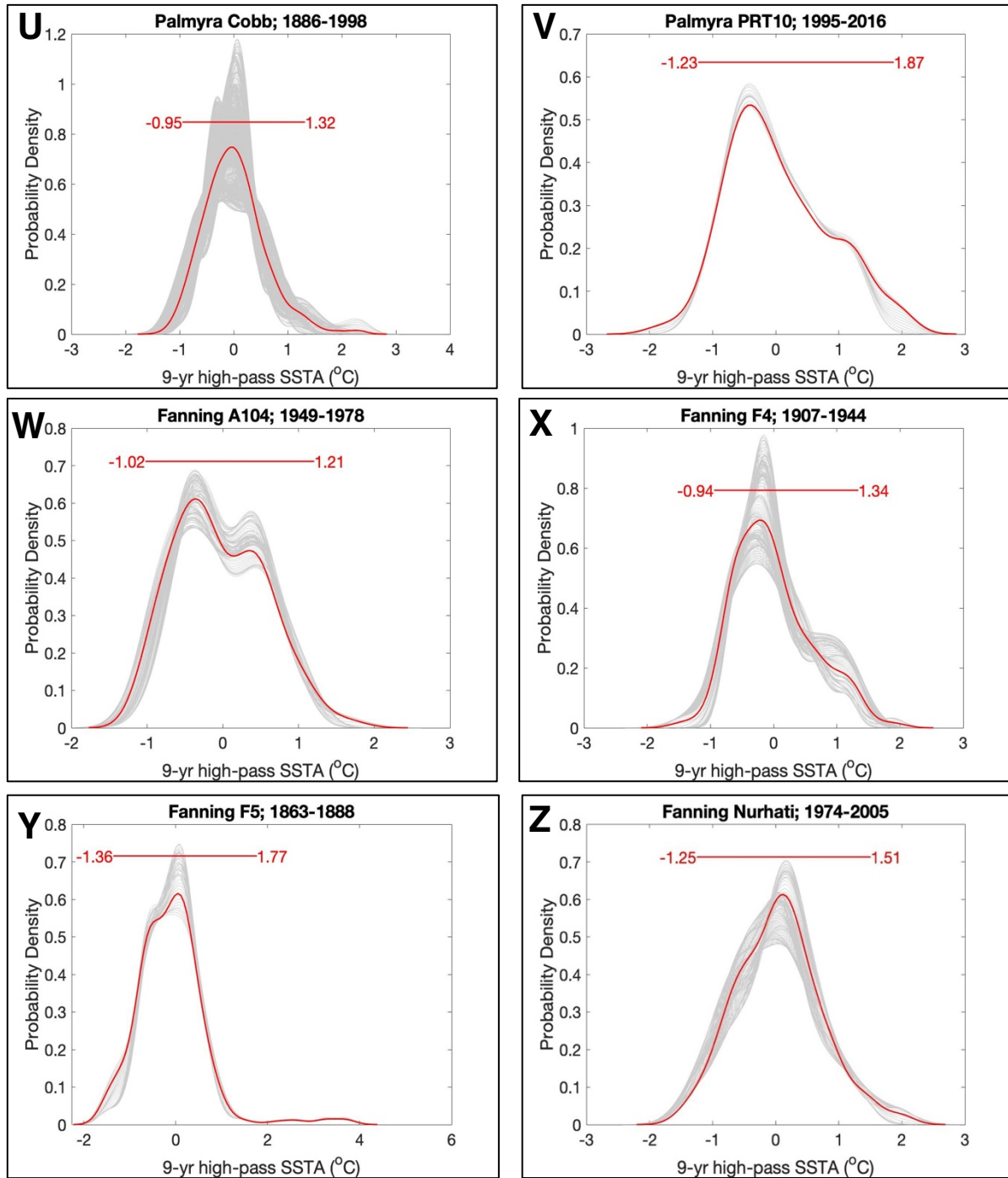


Figure S30-Z. Same as above, but “20th century” coral records from the central Pacific Ocean. Data are taken from Palmyra, Christmas, and Fanning Islands in the Northern Line Islands: **O**) Spliced Palmyra Record (130 yrs; Sanchez et al., 2020); **P**) Spliced Christmas Coral Record (77 yrs; Grothe et al., 2019), **Q**) X12-6 (26 yrs; Grothe et al., 2019), **R**) Christmas Island (26 yrs; Nurhati et al., 2009), **S**) Christmas Island (55 yrs; Evans et al., 1999), **T**) Palmyra Island (26 yrs; Nurhati et al., 2009), **U**) Palmyra Island (112 yrs; Cobb et al., 2001), **V**) PRT10 (21 yrs; Sanchez et al., 2020), **W**) A104 (29 yrs; Cobb et al., 2013), **X**) F4 (37 yrs; Sanchez et al., 2020), **Y**) F5 (25 yrs; Sanchez et al., 2020), **Z**) Fanning Island (31 yrs; Nurhati et al., 2009).

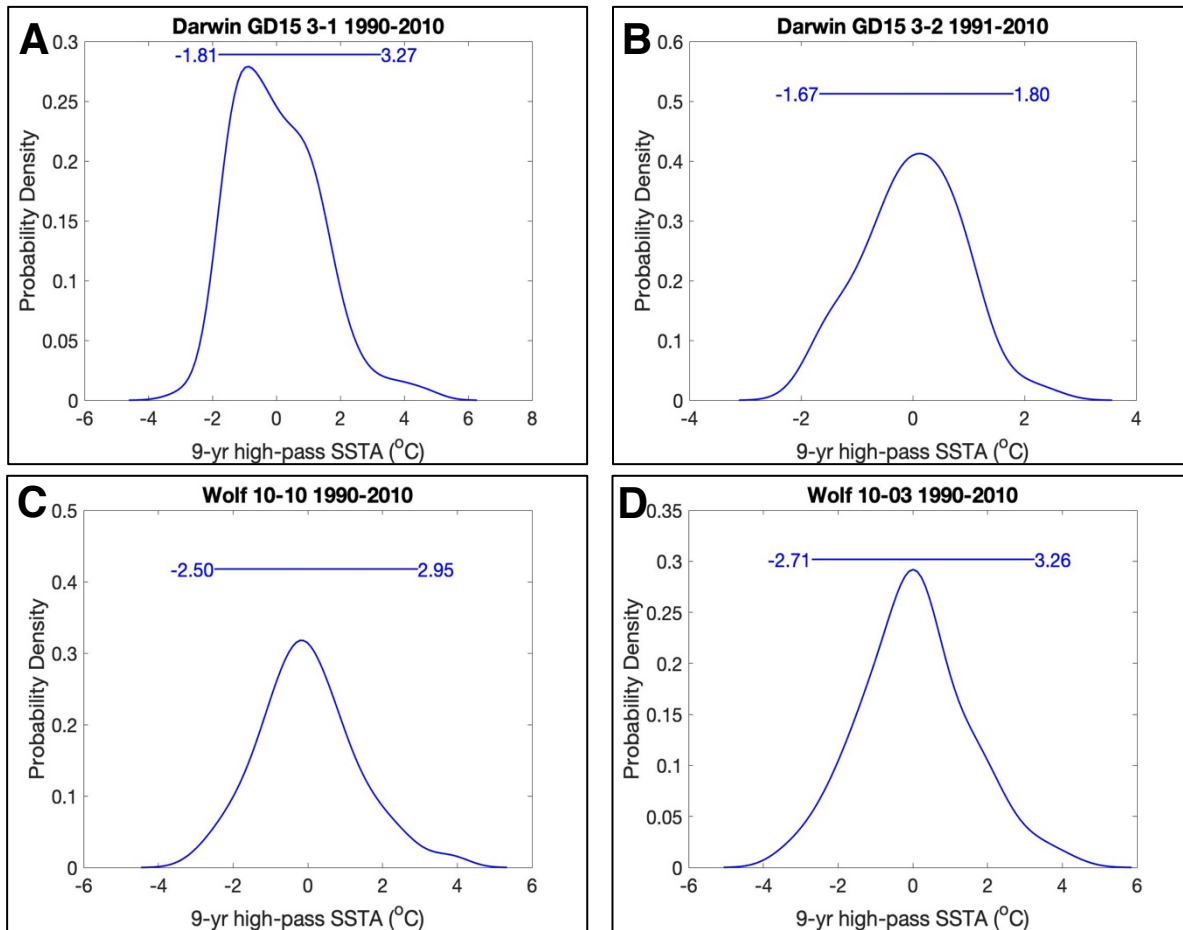


Figure S4A-D. “Recent modern” PDF windows (1990-2010 CE) extracted from modern eastern Pacific coral records. Record GD15 3-2 spans 1991-2010 because the record started in 1991. See table S1A for all original references.

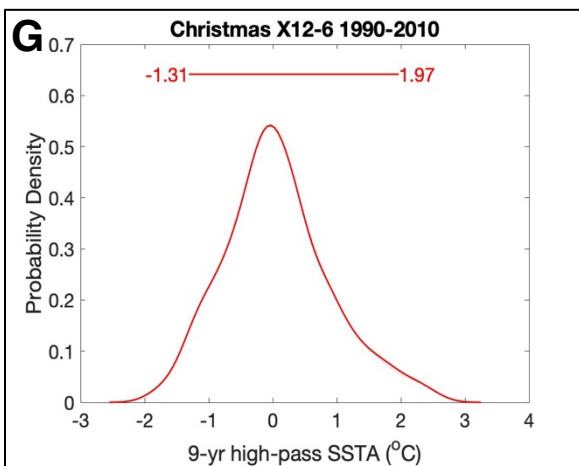
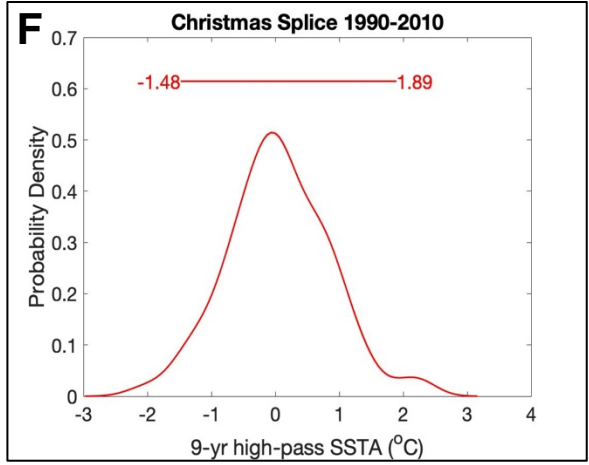
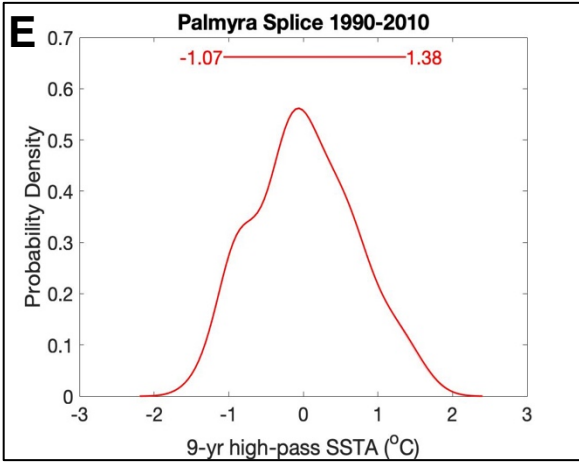


Figure S4E-G. “Recent modern” PDF windows (1990-2010 CE) extracted from modern central Pacific coral records. See table S1B for all original references.

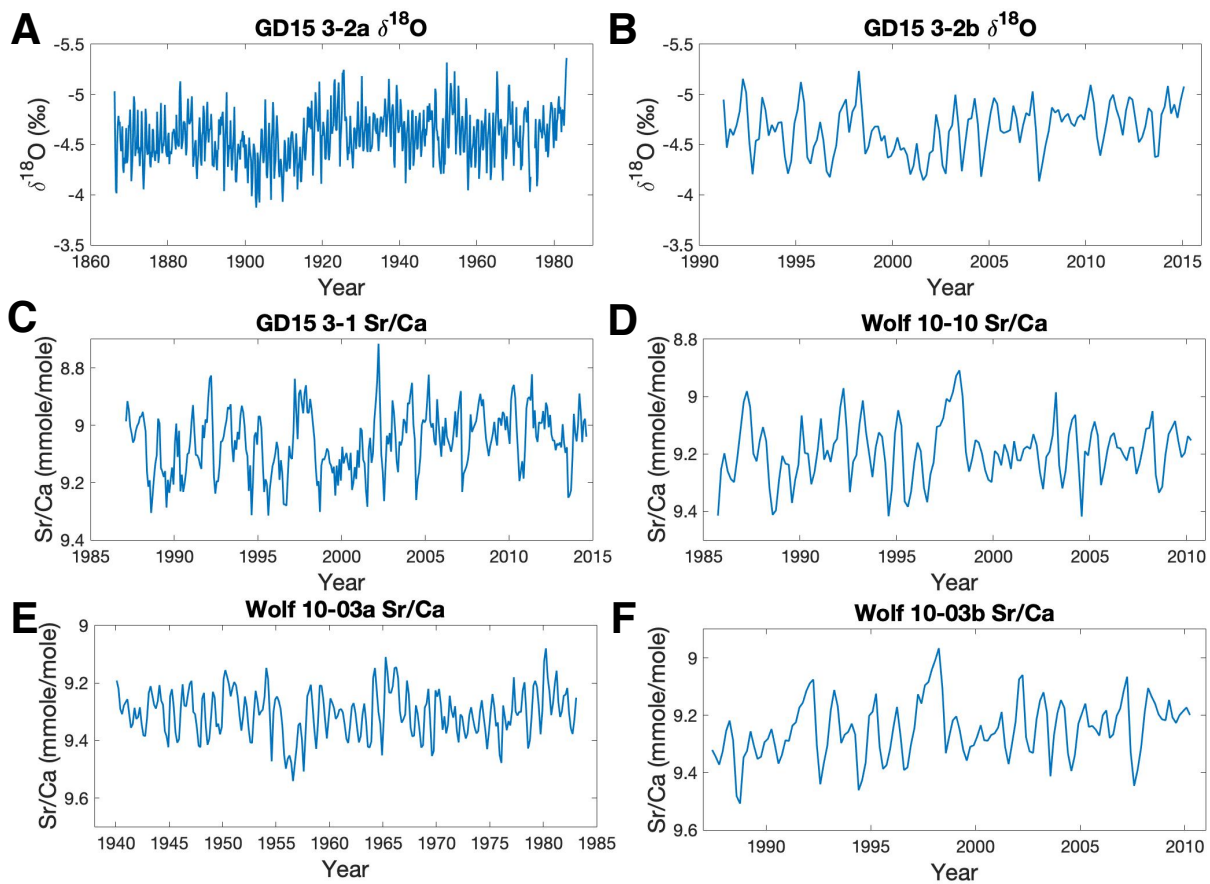


Figure. S5A-F. $\delta^{18}\text{O}$ and Sr/Ca records of modern Galápagos coral records summarized in Table S1A.

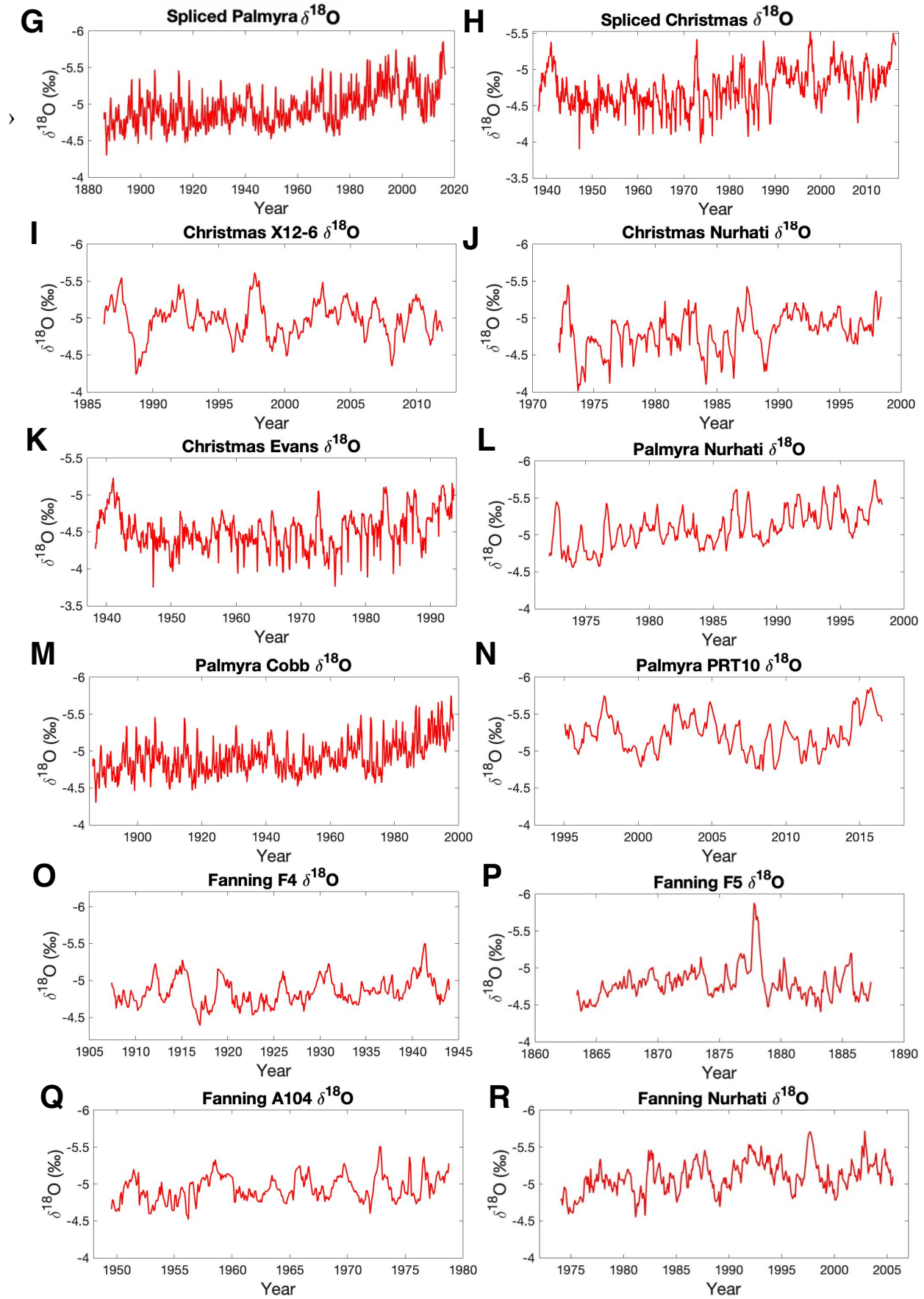


Figure. S5G-R. (From above page) $\delta^{18}\text{O}$ records of modern coral records from the Northern Line Islands, summarized in Table S1B.

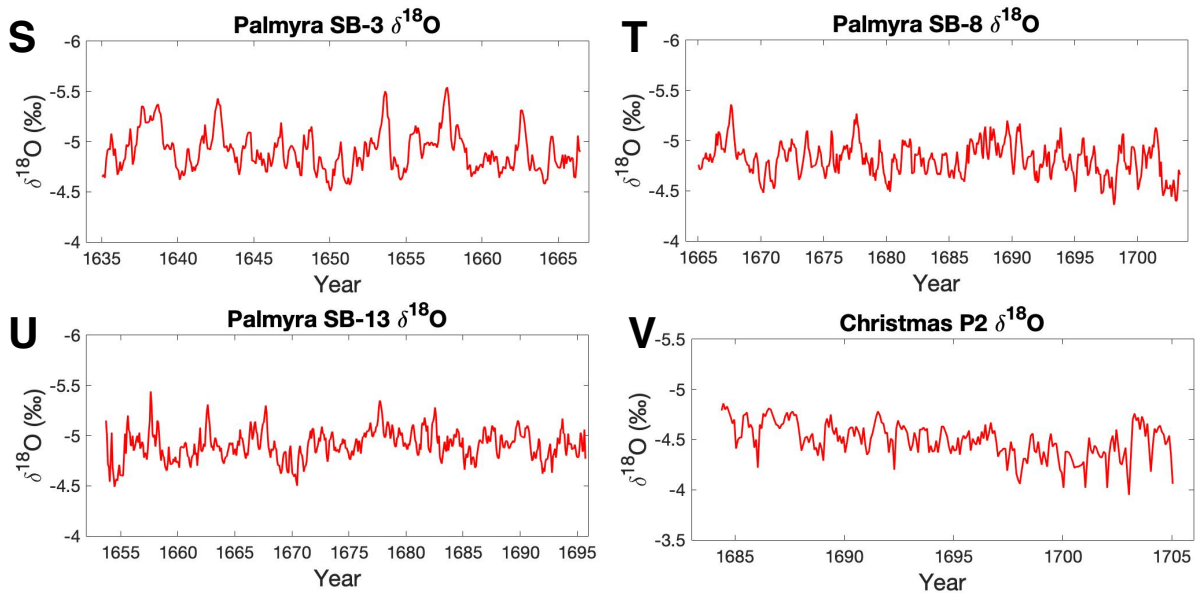


Figure. S5S-V. $\delta^{18}\text{O}$ records of fossil coral records from the Northern Line Islands, summarized in Table S1B.

Table S1A. Summary of the eastern Pacific coral records used in this study. All records are from the Galápagos Islands.

Location	Core Name	Lat/Long	Fossil/Modern	$\delta^{18}\text{O}$ or Sr/Ca	Record Length	Citation	Notes
Genovesa Island	GEN-16-1	0.3231°N, 89.9580°W	Fossil	$\delta^{18}\text{O}$	1678-1710; 32 yrs.	This study.	—
Genovesa Island	GEN-16-3	0.3231°N, 89.9580°W	Fossil	$\delta^{18}\text{O}$	1758-1781; 23 yrs.	This study	—
Urvina Bay	UR-86	-0.25°N, -91.367°W	Fossil	$\delta^{18}\text{O}$	1783-1835; 52 yrs.	Modified from Druffel et al., 2015	Record was re-age modeled.
Wolf Island	10-04	1.3836°N, 91.8160°W	Fossil	Sr/Ca	1693-1776; 83 yrs	Modified from Reed et al., 2021	—
Darwin Island	GD15 3-2a	1.6787°N, 92.0041°W	Modern	$\delta^{18}\text{O}$	1866-1983; 117 yrs.	Jimenez, 2019	Death horizon spanning 1983-1991.
Darwin Island	GD15 3-2b	1.6787°N, 92.0041°W	Modern	$\delta^{18}\text{O}$	1991-2015; 24 yrs.	Jimenez, 2019	Core above death horizon
Darwin Island	GD15 3-1	1.6787°N, 92.0041°W	Modern	Sr/Ca	1987-2014; 27 yrs.	Cheung et al., <i>unpublished</i>	—
Wolf Island	10-10	1.3836°N, 91.8160°W	Modern	Sr/Ca	1985-2015; 30 yrs.	Jimenez et al., 2018	—
Wolf Island	10-03a	1.3836°N, 91.8160°W	Modern	Sr/Ca	1940-1983; 43 yrs.	Jimenez et al., 2018	Death horizon from 1983-1987.
Wolf Island	10-03b	1.3836°N, 91.8160°W	Modern	Sr/Ca	1987-2010; 23 yrs	Jimenez et al., 2018	Core above death horizon.

Table S1B. Summary of the central Pacific coral records used in this study. All records are from the Northern Line Islands.

Location	Core Name	Lat/Long	Fossil/Modern	$\delta^{18}\text{O}$ or Sr/Ca	Record Length	Citation	Notes
Palmyra Island	Sb-3	5.8885°N, 162.0787°W	Fossil	$\delta^{18}\text{O}$	1635- 1666; 31 yrs.	Cobb et al., 2013	—
Palmyra Island	Sb-13	5.8885°N, 162.0787°W	Fossil	$\delta^{18}\text{O}$	1653- 1695; 42 yrs.	Cobb et al., 2013	—
Palmyra Island	Sb-8	5.8885°N, 162.0787°W	Fossil	$\delta^{18}\text{O}$	1665- 1703; 38 yrs.	Cobb et al., 2013	—
Christmas Island	P2	1.8721°N, 157.4278°W	Fossil	$\delta^{18}\text{O}$	1684- 1705; 21 yrs.	Cobb et al., 2013	—
Spliced Palmyra Island	Spliced Palmyra Coral Record	5.8885°N, 162.0787°W	Modern	$\delta^{18}\text{O}$	1886- 2016; 130 yrs.	Sanchez et al., 2020	1990-2010 standard deviation used to define modern interval
Spliced Christmas Island	Spliced Christmas Coral Record	1.8721°N, 157.4278°W	Modern	$\delta^{18}\text{O}$	1939- 2016; 77 yrs.	Grothe et al., 2019	1990-2010 standard deviation used to define modern interval
Christmas Island	X12-6	1.8721°N, 157.4278°W	Modern	$\delta^{18}\text{O}$	1986- 2012; 26 yrs.	Grothe et al., 2019	—
Christmas Island	Christmas Island (Nurhati)	1.8721°N, 157.4278°W	Modern	$\delta^{18}\text{O}$	1972- 1998; 26 yrs.	Nurhati et al., 2009	—
Christmas Island	Christmas Island (Evans)	1.8721°N, 157.4278°W	Modern	$\delta^{18}\text{O}$	1938- 1993; 55 yrs.	Evans et al., 1999	—
Palmyra Island	Palmyra Island (Nurhati)	5.8885°N, 162.0787°W	Modern	$\delta^{18}\text{O}$	1972- 1998; 26 yrs.	Nurhati et al., 2009	—
Palmyra Island	Palmyra Island (Cobb)	5.8885°N, 162.0787°W	Modern	$\delta^{18}\text{O}$	1886- 1998; 112 yrs.	Cobb et al., 2001	—
Palmyra Island	PRT10	5.8885°N, 162.0787°W	Modern	$\delta^{18}\text{O}$	1995- 2016; 21 yrs.	Sanchez et al., 2020	—

Fanning Island	A104	3.8743°N, 159.3191°W	Modern	$\delta^{18}\text{O}$	1949- 1978; 29 yrs.	Cobb et al., 2013	—
Fanning island	F4	3.8743°N, 159.3191°W	Modern	$\delta^{18}\text{O}$	1907- 1944; 37 yrs.	Sanchez et al., 2020	—
Fanning Island	F5	3.8743°N, 159.3191°W	Modern	$\delta^{18}\text{O}$	1863- 1888; 25 yrs.	Sanchez et al., 2020	—
Fanning Island	Fanning Island (Nurhati)	3.8743°N, 159.3191°W	Modern	$\delta^{18}\text{O}$	1974- 2005; 31 yrs.	Nurhati et al., 2009	—

S2A-B. List of temperature conversions used to calculate SST from $\delta^{18}\text{O}$ or Sr/Ca values in **A)** eastern or **B)** central Pacific coral records.

A

Record	Temperature Conversion Used
GEN-16	x/-0.2
Urvina Bay	x/-0.2
Darwin GD15 3-2	x/-0.135
Wolf 10-04	x/-0.061
Darwin GD15 3-1	x/-0.053
Wolf 10-10	x/-0.061
Wolf 10-03	x/-0.058

B

Record	Temperature Conversion Used
Palmyra SB-3	x/-0.2
Palmyra SB-13	x/-0.2
Palmyra SB-8	x/-0.2
Christmas p2	x/-0.2
Spliced Palmyra	x/-0.2
Spliced Christmas	x/-0.2
X12-6	x/-0.2
Christmas Nurhati	x/-0.2
Christmas Evans	x/-0.2
Palmyra Nurhati	x/-0.2
Palmyra Cobb	x/-0.2
PRT10	x/-0.2
A104	x/-0.2
F4	x/-0.2
F5	x/-0.2
Fanning Nurhati	x/-0.2

Table S3A. PDF distribution spreads of fossil coral records from the eastern Pacific Ocean. “Spread” refers to the distance between the 2.5th and 97.5th percentile of SSTAs. **Average Spread: 2.94**

Fossil Eastern Pacific Coral Record; 17th-18th Century	PDF Distribution Spread
Genovesa 1	3.0
Genovesa 3	2.54
Urvina Bay	2.59
Wolf Island	3.61

Table S3B. Same above, but PDF distribution spreads of 20th century and extracted recent modern coral records from the eastern Pacific Ocean. **Average Spread: 4.83 (*Modern interval spreads not included in this average).**

Modern Eastern Pacific Coral Record; 20th-21st Century	PDF Distribution Spread
Darwin Island GD15 3-2a	3.47
Darwin Island GD15 3-2b	3.40
Darwin Island GD15 3-1	5.57
Wolf Island 10-10	6.31
Wolf Island 10-03a	4.4
Wolf Island 10-03b	5.88
*Wolf 10-10 Recent Modern (1990-2010)	5.45
*Wolf 10-03 Recent Modern (1990-2010)	5.97
*Darwin GD15 3-1 Recent Modern (1990-2010)	5.08
*GD15 3-2 Recent Modern (1990-2010)	3.47

Table S3C. Same above, but PDF distribution spreads of fossil coral records from the central Pacific Ocean. **Average Spread: 2.17**

Fossil Central Pacific Coral Record; 17th-18th Century	PDF Distribution Spread
Palmyra Island sb-3	2.59
Palmyra Island sb-13	2.19
Palmyra Island sb-8	1.83
Christmas Island p2	2.07

Table S3D. Same above, but PDF distribution spreads of 20th century and extracted recent modern coral records from the central Pacific Ocean. **Average Spread: 2.86 (*Spliced records and recent modern interval spreads not included in this average).**

Modern Central Pacific Coral Record; 20th-21st Century	PDF Distribution Spread
*Spliced Palmyra	2.38
*Spliced Christmas	3.15
X12-6	3.68
Christmas Nurhati	3.91
Christmas Evans	2.64
Palmyra Nurhati	2.61
Palmyra Cobb	2.27
PRT10	3.10
A104	2.23
F4	2.28
F5	3.13
Fanning Nurhati	2.76
*Spliced Palmyra Recent Modern (1990-2010)	2.45
*Spliced Christmas Recent Modern (1990-2010)	3.37
*X12-6 Recent Modern (1990-2010)	3.28